Speed Control of Permanent Magnet Synchronous Motor using Vector Control for Electric Vehicle

Name of Candidate: **Terefe Taye Mesfin**

A Thesis Submitted to:

The Department of Power and Control Engineering

School of Electrical Engineering and Computing

Presented in Partial Fulfilment of the Requirement for the Degree in Power Electronics

Office of Graduate Studies
Adama Science and Technology University

Adama
February, 2019

Speed Control of Permanent Magnet Synchronous Motor using Vector Control for Electric Vehicle

Name of Candidate: **Terefe Taye Mesfin**

Advisor: **Dr. K V L Narayana**
Co-Advisor: **Dr. Kemal Ibrahim**

A Thesis Submitted to:

The Department of Power and Control Engineering

School of Electrical Engineering and Computing

Presented in Partial Fulfilment of the Requirement for the Degree in
Power Electronics

Office of Graduate Studies
Adama Science and Technology University

Adama
February, 2019

Approval of Board of Examiners

We, the undersigned, members of the Board of Examiners of the final open defense by ________________________________ have read and evaluated his thesis entitled **Speed Control of Permanent Magnet Synchronous Motor using Vector Control for Electric Vehicle** and examined the candidate. This is, therefore, to certify that the thesis has been accepted in partial fulfillment of the requirement of the Degree of : . . . .

Dr.K V L Narayana		02-05-2019
Advisor	Signature	Date
Chairperson	Signature	Date
Internal Examiner	Signature	Date
External Examiner	Signature	Date

Approval Sheet

Name of student	Signature	Date
Dr.K V L Narayana		02-05-2019
Advisor	Signature	Date
Department Chair	Signature	Date
School Dean	Signature	Date
Postgraduate Dean	Signature	Date

Adviser's Approval Sheet

To : **Power and Control Program** Department

Subject : Thesis Submission

This is to certify that the thesis entitled **Speed Control of Permanent Magnet Synchronous Motor using Vector Control for Electric Vehicle** Submitted in partial fulfillment of the requirements for the Degree of Masters in **Power Electronics** , the Graduate program of the department of **Power and Control engineering**, and has been carried out by **Terefe Taye Mesfin, Id.No: R/0051/09**, under my supervision. Therefore, I recommend that the student has fulfilled the requirements and hence hereby he can submit the thesis to the department.

Dr.K V L Narayana		02-05-2019
Name of major Advisor	Signature	Date

Declaration

I hereby declare that this MSc Thesis is my original work and has not been presented for a degree in any other university, and all sources of material used for this thesis have been duly acknowledged.

Name : ____________________

Signature : ____________________

This MSc/ MA Thesis has been submitted for examination with my approval as thesis advisor.

Name : Dr.K V L Narayana

Signature : ____________________

Date of submission : 06-02-2019

ACKNOWLEDGMENT

I would like to express my deepest thank and gratitude to my advisor Dr. K V L Narayana for his advices,and guidance.

I would like to thank my former advisor Prof.kim for his support and guidance.

I would like to express my deepest thanks and gratitude to my Co-advisor Dr. Kemal Ibrahim for his Comment during selecting my thesis title.

Last but not least, I would like to thank my family for their great support during my study.

CONTENTS

List of Tables

List of Figures

LIST OF ACRONYMS

AC : Alternating Current
Back-EMF : Back-Electromotive Force
CTOR : Constant Torque Operation Region
CPOR : Constant Power Operation Region
DC : Direct Current
DTC : Direct Torque Control
EMF : Electromotive Force
EV : Electric Vehicle
FOC : Field Oriented Control
FW : Flux-Weakening
IPMSM : Interior Permanent Magnet Synchronous Motor
MMF : Magnetomotive Force
MTPA : Maximum Torque per Ampere
PM : Permanent Magnet
PMSM : Permanent Magnet Synchronous Motor
PI : Proportional Integral
PWM : Pulse Width Modulation
RPM : Revolutions per minute
SPWM : Sinusoidal Pulsewidth Modulation
SRM : Switch Reluctance Motor
VSI : Voltage Source Inverter

Abstract

This thesis focused on the control of PMSM using vector control(FOC) method with field weakening Techniques for Three Wheel electric vehicle (EV) application .A PMSM motor model has been Studied and analyzed to control the motor both in the constant-torque (constant flux) and in the constant power (flux weakening) regions.The objective of the field weakening technique is then to control i_d *and* i_q *current in such way that the motor can develop constant power and achieved wide speed range operation.Surface mounted PMSM have been used in this thesis that is* $L_q = L_d$ *so that reluctance torque due to inductance considered as zero.The analysis of Vector controled flux weakening techniques PMSM drive system shows that the armature current is controlled to have a field component that weakens the air gap field, and therefore opposes the back emf. However, the armature current vector must satisfy the voltage and current constraints. Due to the upper limit set on the available dc link voltage and current ratings of a given inverter are limited.The voltage and current limit affect both the maximum speed and rated torque operation.So that inorder to achieved those constraint flux weakening have been applied in constan power operation region.The simulation result have been showed that the speed range improved from 3900RPM(base speed) to 5000Rpm(Maximum speed).Therefor the result showed that using flux weakining method we could increased the speed range with in desired power rating of the motor.*

Keywords:- PMSM, Vector Control, FOC,Field Weakening,EV.

CHAPTER 1:

INTRODUCTION

1.1 Background

Electric vehicles (EVs) have become more and more attractive in recent years, as they are considered as the most viable solution to help protect the environment and to achieve high energy efficiency for transportation[2].In EVs, traction motors are the key component for propulsion which requires high torque and power density, wide speed range, high efficiency, high reliability,low noise, and reasonable cost.Hence Permanent Magnet Synchronous Motors (PMSM) are attracting growing attention for a wide variety of industrial applications, from simple applications like pumps or fans to high performance drives like Electric vehicles(EV's) . This is due to their main characteristics: high power density, high torque to inertia ratio and high efficiency. Permanent magnet motors are double excited electric machines. The first source of excitation is the field of the permanent magnet situated in the rotor, while the second source is the field produced by the stator winding when supplied with a 3-phased voltage system[1]. Induction motor have been the most prevalent electric motor in the twentieth century. As of late, attributable to the quick advancement made in the field of power electronics and control innovation, the applications of induction motors to electrical drives have expanded. The principle focal points of induction motors are their easier construction, simple maintenance, no commutator or slip rings, low cost and high reliability. The weaknesses are their lower efficiency and poorer power factor than PM motor. The utilization of PM motors in electrical drives has turned into progressively attractive choice than induction motors. The enhancements made in the field of semiconductor drives imply that the control of PM motors has turned out to be easier and cost effective with the likelihood of working the motor over a wide speed range and as yet keeping up a good efficiency and power factor.

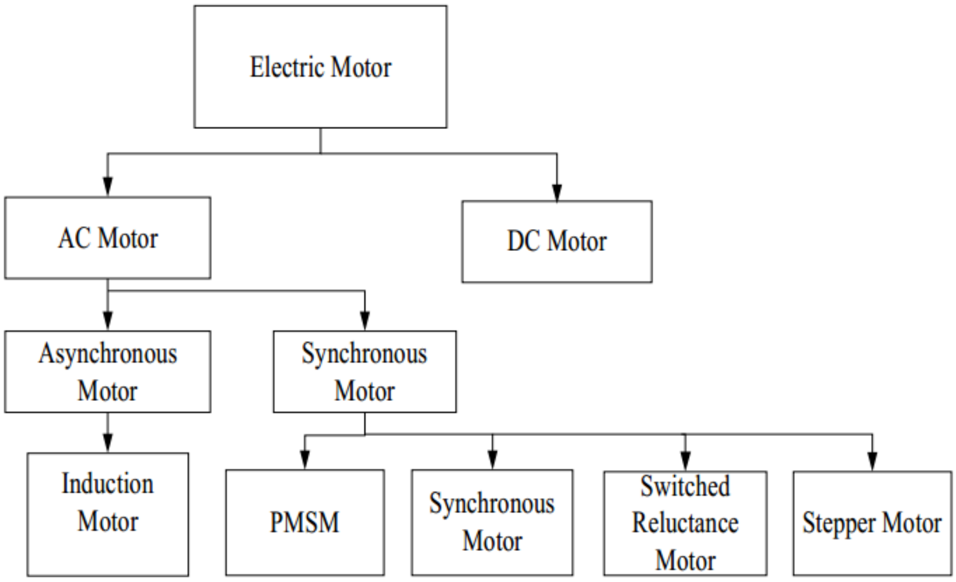

Figure 1.1: General Classifications of Electric Motors

1.2 Classification of Permanent Magnet Motors

PM motors are classified on the basis of the flux density distribution and the shape of current excitation. They are Permanent Magnet Synchronous Motors (PMSM) and Permanent Magnet Brushless DC Motors (BLDC). The PMSM has a sinusoidal-shaped back EMF and is designed to develop sinusoidal back EMF waveforms. They have the following features:

- Sinusoidal distribution of magnet flux in the air gap
- Sinusoidal current waveforms

BLDC has a trapezoidal-shaped back EMF and is designed to develop trapezoidal back EMF waveforms. They have the following features:

- Rectangular distribution of magnet flux in the air gap
- Rectangular current waveform

This thesis is focused on the Permanent Magnet Synchronous Motors (PMSM).

1.3 Classification of Permanent Magnet Synchronous Motor (PMSM)

The PMSM consists of a three phase stator similar to that of an induction motor and a rotor with permanent magnets. Most of the PMSM drives arc fed from inverters. The motor characteristics depend on the type of the magnets used and the way they are located on the rotor. The magnets are either mounted on the surface of the rotor or buried in the interior of the rotor. Accordingly PMSMs are classified as

1. Surface mounted PMSMs

2. Buried or interior PMSMs

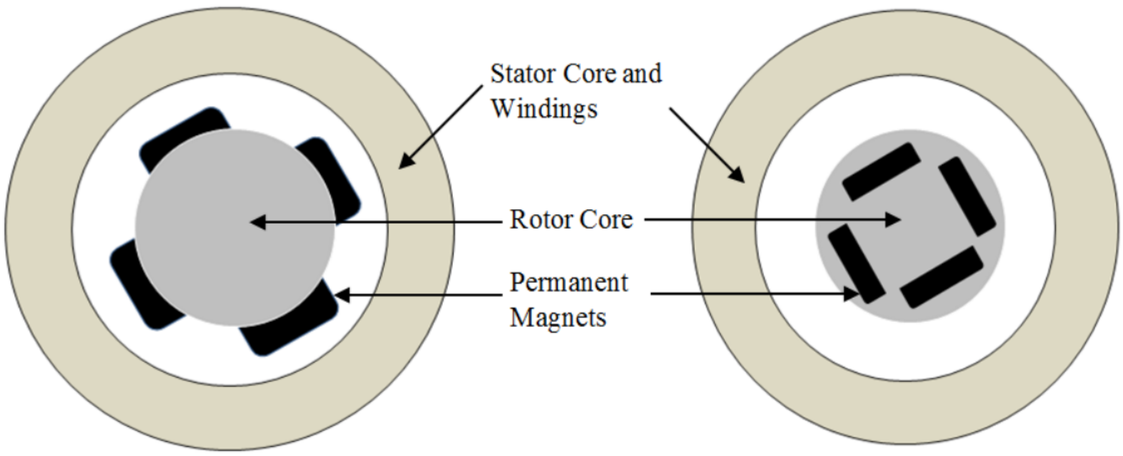

(a)Surface mounted magnet (b)Interior mounted magnet

Figure 1.2: Rotor configuration of PMSM (a) surface mounted (b) interior mounted[9]

1. Surface mounted PMSMs

Surface mounted PM motors have each of the permanent magnets mounted on the surface of the rotor, making it easy to build.This configuration is used for medium speed applications because of the limitation that the magnets will fly apart during high-speed operations.These motors are considered to have insignificant saliency, thus having practically equal inductances in both the q and d axes [3]. The ratio between the quadrature and direct axis inductances is close to one i.e.,$L_q = L_d$. The rotor has an iron core that may be solid or may be made of punched laminations for simplicity in manufacturing[3,6].Thin permanent magnets are mounted on the surface of this core using adhesives. Alternating magnets of the opposite magnetization direction produce radially directed flux density across the air gap. This flux density then interacts with currents in windings placed in slots on the inner surface of the stator to produce torque.

2. Interior PMSMs

Interior PM motors, on the other hand, have interior mounted permanent magnet rotor as shown in figure 1.1(b).Permanent magnet is mounted inside the rotor.Because of the internal positioning of the rotor magnets, it is good for high-speed operation.These motors are considered to have saliency with q-axis inductance greater than the d-axis inductance, $L_q > L_d$. The magnets are very well protected against centrifugal forces [6].The high ratio between the quadrature and direct axis inductances in the interior PMSM is a boost for the electromagnetic torque by bringing in the reluctance torque.

1.4 Statement of the Problem

In Ethiopia almost all three-wheel vehicles are internal combustion engine(ICE) and this ICE consumes petroleum and our dependency on petroleum venerable us for price spike and supply disruption.So in thesis thesis I have changed ICE engines by electric motor(PMSM) for three wheels vehicles which uses domestically produced electricity .

1.5 General and Specific Objective

General Objective

The general objective of this thesis is speed control of PMSM using vector control method which is suitable for wide speed range operation using field-weakening approach for electric vehicle application.

Specific Objectives are To:

- Study and develop vector control algorithm for PMSM speed control
- Model and simulate PMSM.
- Achive wide speed range operation using flux weakening approach

1.6 Scope of Study

The scope of this thesis includes mathematical modeling,simulation and analysis of three phase permanent magnet synchronous motor(Surface mounted PMSM) for small electric vehicle.

1.7 Significant of study

Almost all vehicle in Ethiopia are IC Engines vehicle which consumes petroleum and our reliance on petroleum makes us vulnerable to price spikes and supply disruptions.EVs help reduce this threat because almost all electricity is generated from domestic sources, including hydro power,and renewable sources.EVs can also reduce the emissions that contribute to climate change and improving public health and reducing ecological damage. So electric vehicle will be a grate option for our future development.Therefore, this study is focused on speed control of PMSM using vector control for EV'S application which is replaced the petrol drive IC engines.

CHAPTER 2:

LITERATURE REVIEW

PMSM's control can be performed in several forms. The most common types can be gathered in two main groups: scalar control and vector control. In permanent magnets motors, the most used scalar control is constant V/f(volt per frequency control). However, due to the poor results obtained in transient state, control imprecisions and phase control limitations, this type of control is becoming less used.To overcome the obstacles imposed by the scalar control and achieve higher performances, vector control is adopted. Here, two main approaches are known: Direct Torque and Flux Control (DTFC), also called Direct Torque Control (DTC), and Field-Oriented Control (FOC). Both DTC and FOC are strategies that allow torque and flux to be decoupled and controlled independently[3].Unlike FOC, in DTC there is no current loop in the control Instead, torque and flux are measured or estimated and the control loop is closed by the inverters control signals from this data [4].Field-Oriented Control can be direct or indirect. Since there is no common agreement in the literature in how to distinguish between them, it is assumed that indirect FOC is based on the estimation of the flux position through stator currents and voltages and motors parameters, whereas direct FOC measures the rotor flux position, usually by Hall sensors[21].There are also current control strategies called Trapezoidal (Six-Step) Current Control and Sinusoidal Current Control. These differ by the form of the current injected in the motor: the first one tries to inject rectangular current waveforms and is usually implemented in BLDC(Brush-less DC Motor) motors. The goal is to feed the appropriate phase of the stator in order to maintain a rotating field. The phase shift between stator and rotor fluxes must be controlled in order to produce the required torque. Sinusoidal Current Control is similar to the previous, except the currents generated are sinusoidal instead of rectangular[10].

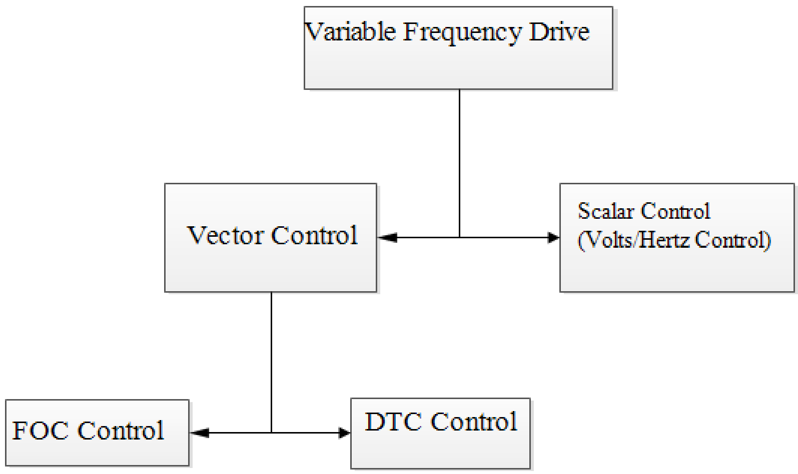

Figure 2.1: Motor control classification.

Table 2.1: Comparison of Vector control

	DTC	FOC
Dynamic response	Excellent	Excellent
Torque ripple	- Indirectly controlled by stator currents - High dynamics - Torque ripple	- Directly controlled - High dynamics - Controlled torque ripple
Average torque controlled	No	Yes(indirect)
Complexity of architecture	Low	Medium
Current distortion and harmonics	High	Medium
Fixed switching frequency	No	Yes
Flux control	Indirectly controlled by stator currents and Slow dynamics	Directly controlled - Fast dynamics
Parameter sensitivity	Low	Medium

Lastly, with respect to methods of electric motoring control used nowadays, five vector control methods commonly applied to drive PMSMs are exposed, with a brief explanation of each [3].

1. **Constant Torque angle control**

    - Torque angle is maintained at 90^o turning if current component into zero.
    - It is used to speeds below rated speed.
    - Power factor decreases with the increase of rotors speed and stator currents.

2. **Unit power factor control[10]**

    - Unit power factor control implies that the VA ratio of the inverter is completely used to inject real power in the motor..
    - This type of control is applied controlling the torque angle as a function of motors variables and is independent of motors speed. used to inject real power in the motor.
    - The torque angle has to be higher than 90^o.

3. **Constant air-gap flux linkage control[3]**

    - The flux that results of stator current dq components and rotor flux, known as mutual or air-gap flux, is kept constant, usually in a value that is equal to the rotor flux.
    - The stator voltage requirements are kept low.
    - It is a simple method to apply flux-weakening, allowing the motor to operate with speeds above the base speed.
    - Torque angle has to be higher than 90^o.

4. **Maximum Torque per Ampere control[3]**

    - Precious control method from machine and inverter usage point of view.
    - It is done controlling the torque angle.
    - Better performance than constant torque angle control, at the expense of higher stator voltages.

5. **Flux-Weakening control[3]**

   - Voltage and current limits imposed by DC bus before the inverter make the motors feeding also limited. This makes the speed and torque produced by the motor also limited. In some applications is necessary to have higher speeds than the maxim speed permitted by the voltage and current fed to the motor.
   - In order to increase the speed, air-gap fluxes are weakened making the electromotive force produced by the rotor inferior to the voltage applied.
   - Flux-weakening is made to be inversely proportional to the stator frequency.

In addition to high torque requirements at low speeds, traction applications require drive systems that provide constant power at high speeds.The drive must be able to maintain the constant power over a wide speed range [9].The speed of the motor increases with the terminal voltage up until the base speed. At base speed the terminal voltage saturates to its maximum value. The speed of the motor cannot be increased any further unless a proper control strategy is implemented to reduce the stator flux. If a demagnetizing magnetomotive force (MMF) generated by manipulation of stator currents is applied, the apparent MMF generated by PMs could be reduced and the motor speed will increase. The strategy is known as field-weakening (FW). Since high power density, high efficiency PM motors have become the best replacements of internal combustion engines, the control of PM motors for EV applications has drawn much attention in recent publications [12]. It is necessary for Evs as well as many other applications, to operate over both a wide speed range and high efficiency. Therefore, a control strategy, which uses FW control at high speed, was demonstrated in [11].
R. Krishnan [32] reviewed the operation of the Permanent Magnet Synchronous Motor Drives when they are constrained to be within the permissible envelope of maximum inverter voltage and current to produce the rated power and to provide this with the highest attainable rotor speed. The rated power is for steady state operation and multiple times that is preferred for fast accelerations and decelerations during transient operation. Effective current control during the field weakening operation with transient capability was seen as preferable compared to the saturation of the current loop resulting in higher peak currents and hence higher copper losses. The paper addressed

the steady state operation, transient operation, and control techniques for the PMSM drives in the field weakening region.

Zordan, Vas, Rashed, Bolognani, and Zigliotto [33] performed a comparative analysis of field-weakening (FW) in vector controlled and DTC permanent magnet synchronous motor drives. The possibility of unstable operation in the highspeed region using DTC was emphasised. The paper also highlighted some important differences between DTC and FOC drives in FW, such as quickness of torque response and torque, flux, current ripple content and implementation aspects.

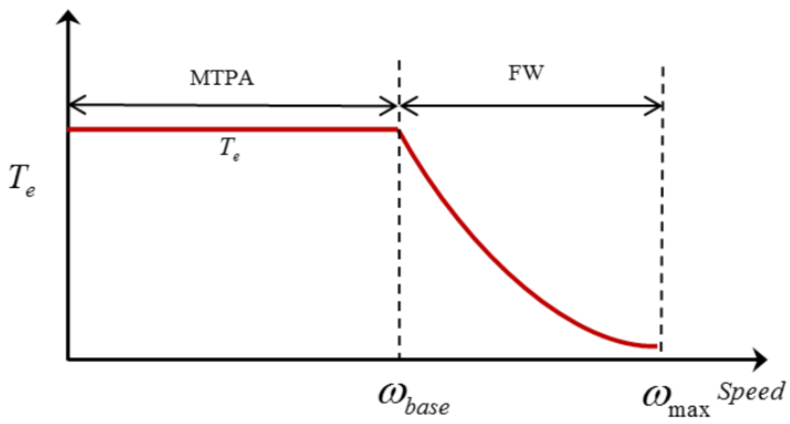

Figure 2.2: Ideal torque vs. speed characteristics for variable speed drives[36].

Generally, as shown in Figure 2.2, MTPA control is achieved with full field current throughout the speed range up to the base speed, which is the maximum speed that can be achieved without FW control [13].Then, in FW control,by injecting negative stator current the armature MMF is re-oriented to a position that opposes the MMF of the PM, and hence reduces the total resultant flux in the airgap. This is the basic idea of the so-called FW control in such machines. The weaker the net resultant air-gap flux the higher the motor speed. That is, in FW control the resultant air-gap flux is in inverse proportion to the motor speed.The principle of FW control in PMSMs is that the air-gap flux can only be weakened by applying a demagnetizing armature current component along the d-axis of the permanent magnets. Since the output torque is proportional to product of air-gap flux and q-axis current component, such torque can be reduced with FW control.

2.1 Comparison of Electric Motor used for EV's Propulsion

There are several types of electric motors can be used in vehicle propulsion systems: DC motors, synchronous motors with permanent magnets or electromagnetic excitation, switched reluctance synchronous motors, squirrel cage induction motors.

Table 2.2: Systems Evaluation of Electric Propulsion[5].

Propulsion System / Characteristics	DC	IM	PM	SRM
Power Density	2.5	3.5	5	3.5
Efficiency	2.5	3.5	5	3.5
Controllability	5	5	4	3
Reliability	5	5	4	3
Technological maturity	5	5	4	3
$\sum$ Total	22	27	25	23

For the same output power, Permanent Magnet Synchronous Motors (PMSM) offer performance enhancement over the induction and synchronous motors in terms of power factor, efficiency, power density and torque-to-inertia ratio [1,2,3].

2.2 PMSM have the following advantages over DC motors

- Higher power density and smaller size
- Sparkless operation (used in hazardous environment)
- Higher speed
- Less audible noise
- Longer life
- Better heat transfer

2.3 PMSM have the following advantages over induction motors

- Higher power density , resulting in smaller size
- Higher efficiency
- Better heat transfer
- Higher power factor

2.4 Demerits of PMSM

- Complex control.
- Demagnetization of the rotor magnet due to ageing.
- Reduction of torque production due to demagnetization of rotor magnet.
- Maintenance is often required for rotor magnet.

2.5 Demand for Three Wheeler Vehicles in Ethiopia

In 2012, Ethiopia imported over 6,920 three wheel vehicles worth 267 million Br, excluding tax. Three years later, imports reached 15,600 vehicles worth 641.2 million Br. In 2016 with in 10 months alone, the country has imported 73,805 three wheel vehicles, which are worth over 817.8 million Br. Their demand is increasing for many reasons,Their affordability in terms of price in comparison to other means of transport and low fuel consumption are some of the reasons behind the rising demand[21].
Data from the Ministry of Transportation indicates that as of last fiscal year 14,793 Bajaj are legally working in Amahara, Afar, Harar, SNNP and Ormia. Of the legally registered vehicles 2,132 are working in Amahara 2,302 in Afar, 536 in Harar,4,671 in SNNP and 5,152 in Oromia. If all of the unlicensed bajaj are included the number could be as high as 200,000[34]. The average import price, excluding local transportation cost, has increased over the years. On average, the price of a three wheel vehicle

in 2012 was around 66,900 birr. In 2016 costs was around 73,805[21]. It now costs over 120,000 birr in 2019.

CHAPTER 3:

MODELING OF PMSM

This chapter deals with the detailed Mathematical modeling of a permanent magnet synchronous motor.As well as Field oriented control of the motor in constant torque and flux-weakening regions are discussed.

3.1 D-Q Modelling of PMSM using Two Phase Machine

The d-q model of Permanent Magnet Synchronous Machine (PMSM) is derived using a two-phase machine in the direct and quadrature axes (dq axes). This approach is desirable because of the conceptual simplicity obtained with only one set of two windings on the stator.The rotor has no winding, only magnets. The magnets are modelled as a flux linkage source concentrating all its flux linkages along only one axis. The physical model of the machine is developed from which the circuit model is derived. The derived model in the stator frame is not suitable for use in analysis as the winding inductances are dependent on the rotor position. Constant inductances for windings are obtained by a transformation to the rotor by replacing the stator windings with a set of fictitious dq windings rotating at arbitrary speed such as the electrical speed of the rotor. The equivalence between the three phase machine and its model using a set of two-phase windings is derived from a simple observation and graphical projection.
The following simplifying assumptions are made to derive the dynamic model of the two-phase PMSM.

i. The stator windings are balanced with sinusoidally distributed magnetomotive force (mmf).

ii. The inductance versus rotor position is sinusoidal.

iii. The saturation and parameter changes are neglected

A two-phase PMSM is shown in Figure 3.1 below. The windings are displaced 90 electrical degrees and the rotor field direction is at an angle r from the stator d -axis winding. The winding current directions and the voltage polarities are shown in detail. A pair of poles is assumed but it is applicable to any number of pair of poles.

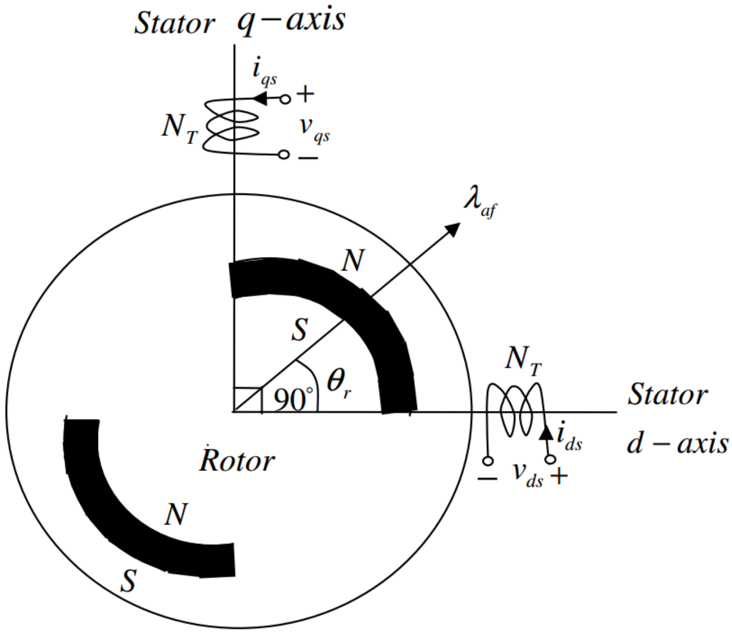

Figure 3.1: Permanent Magnet Synchronous Motor two phase model[3]

The d and q-axis stator voltages are derived as the sum of the resistive voltage drops and the derivatives of the flux linkages in the respective windings as

$$V_{qs} = R_q i_{qs} + p\lambda_{qs} \tag{3.1}$$

$$V_{ds} = R_d i_{ds} + p\lambda_{ds} \tag{3.2}$$

where

p is the differential operator,d/dt

$V_{qs}$and V_{ds} are voltage in the q- and d-axis windings

$i_{qs}$and i_{ds} are the q-and d-axis stator currents

$R_q$and R_d are the stator q- and d-axis resistances

λ_{qs} and λ_{ds} are the stator q- and d-axis sator flux linkages

The stator flux linkage can be written as the sum of the flux linkages due to its self excitation and the mutual flux linkage resulting from other windings and the magnetic sources. Therefore, the q and d axis stator flux linkages are written as:

$$\lambda_{qs} = L_{qq} i_{qs} + L_{qd} i_{ds} + \lambda_{af} \sin(\theta_r) \tag{3.3}$$

$$\lambda_{ds} = L_{dq} i_{qs} + L_{dd} i_{ds} + \lambda_{af} \cos(\theta_r) \tag{3.4}$$

Since the windings are assumed to be balanced, therefore, their resistances are equal and denoted as

$$R_S = R_q = R_d \tag{3.5}$$

Substituting equations 3.3, 3.4, and 3.5 into equations 3.1 and 3.2

$$V_{qs} = R_s i_{qs} + i_{qs} p L_{qq} + L_{qq} p i_{qs} + L_{qd} p i_{ds} + i_{ds} p L_{qd} + \lambda_{af} p \sin(\theta_r) \tag{3.6}$$

$$V_{ds} = R_s i_{ds} + i_{qs} p L_{qd} + L_{qd} p i_{qs} + L_{dd} p i_{ds} + i_{ds} p L_{dd} + \lambda_{af} p \cos(\theta_r) \tag{3.7}$$

L_{qq} and L_{dd} are the self inductances of the q and d axes windings respectively.
L_{qd} is the mutual inductance between q and d axes winding measured on the qaxis.
L_{dq} is the mutual inductance between q and d axes winding measured on the daxis.

3.1.1 Derivation of Inductances as a function of Rotor Position

From figure 3.1, consider the d-axis inductance when the rotor angle $\theta_r = 0$, magnetic axis is aligned with the d-axis and flux linking d-axis coil is maximum thus resulting in d-axis maximum inductance L_d . When $\theta_r = 90^o$,magnetic axis is aligned with q-axis making flux linking d-axis coil minimum thus resulting in d-axis minimum inductance L_q . Because the windings are distributed to provide the sinusoidal mmf, the self inductances can be modelled as cosinusoidal functions of twice the rotor position from the d-axis. Hence the self inductances of the q and d axes windings are written in terms of the maximum winding inductances at the q and d positions as:

$$L_{qq} = \frac{1}{2}\left[(L_q + L_d) + (L_q - L_d)\cos(2\theta_r)\right] \tag{3.8}$$

$$L_{dd} = \frac{1}{2}\left[(L_q + L_d) - (L_q - L_d)\cos(2\theta_r)\right] \tag{3.9}$$

At $\theta_r = 0^o$, $L_{dd} = L_d$ while at $\theta_r = 90^o$, $L_{dd} = L_q$ in accordance with the discussion above.

In compact form

$$L_{qq} = L_1 + L_2 \cos(2\theta_r) \tag{3.10}$$

$$L_{dd} = L_1 - L_2 \cos(2\theta_r) \tag{3.11}$$

Where L_1 and L_2 are given as

$$L_1 = \frac{1}{2}(L_q + L_d) \tag{3.12}$$

$$L_2 = \frac{1}{2}(L_q - L_d) \tag{3.13}$$

The mutual inductance between the q and d axis is zero in a cylindrical rotor machine. In an interior PMSM, there is saliency and because of that a part of the d-axis winding flux will link the q-axis winding as the uneven reluctance provides a path for flux through the q-axis. The mutual coupling is zero when rotor position is 0^o and 90^o and maximum at -45^o. Assuming sinusoidal variation, the mutual inductance between q and d axes windings is given by:

$$L_{qd} = \frac{1}{2} = (L_q - L_d)\sin(2\theta_r) = -L_2 \sin(2\theta_r) \tag{3.14}$$

Substituting the self and mutual inductance (i.e. equations 3.8, 3.19 and 3.14) into the stator voltage equation (i.e. equations 3.6 and 3.7) and rearranging in compact form yields

$$\begin{bmatrix} V_{qs} \\ V_{ds} \end{bmatrix} = R_s \begin{bmatrix} 2i_{qs} \\ i_{ds} \end{bmatrix} + \begin{bmatrix} L_1 + L_2 \cos 2\theta_r & -L_2 \sin 2\theta_r \\ -L_2 \sin 2\theta_r & L_1 - L_2 \cos 2\theta_r \end{bmatrix} \frac{d}{dt} \begin{bmatrix} i_{qs} \\ i_{ds} \end{bmatrix} \tag{3.15}$$

$$+2\omega_r L_2 \begin{bmatrix} -\sin 2\theta_r & -\cos 2\theta_r \\ -\cos 2\theta_r & \sin 2\theta_r \end{bmatrix} \begin{bmatrix} i_{qs} \\ i_{ds} \end{bmatrix} + \lambda_{af}\omega_r \begin{bmatrix} \cos\theta_r \\ -\sin\theta_r \end{bmatrix}$$

The third term as well as the position-dependent elements in the second term exist because of saliency in Interior Permanent Magnet Synchronous Machines being that $L_q \neq L_d$. In surface mounted machines, $L_q = L_d$ thus $L_2 = 0$. The stator voltage equations, therefore, minimize to

$$\begin{bmatrix} V_{qs} \\ V_{ds} \end{bmatrix} = R_s \begin{bmatrix} 2i_{qs} \\ i_{ds} \end{bmatrix} + \begin{bmatrix} L_1 & 0 \\ 0 & L_1 \end{bmatrix} \frac{d}{dt} \begin{bmatrix} i_{qs} \\ i_{ds} \end{bmatrix} + \lambda_{af}\omega_r \begin{bmatrix} \cos\theta_r \\ -\sin\theta_r \end{bmatrix} \tag{3.16}$$

The inductances in the salient pole machines (interior PMSM) are rotorposition dependent making the voltage equations cumbersome and not providing insight into the machine steady state and dynamic behaviour. Transformation techniques are used to eliminate this rotor dependency since it is more popular for steady state and dynamic studies of the machine to be conducted with inductances independent of rotor position. The next subsection is devoted to the transformation to rotor reference frame.

3.1.2 Transformation to Rotor Reference Frame

By transforming to the rotor reference frame, the system inductance matrix becomes independent of the rotor position, thus leading to the simplification and compactness of system equations. The relationship between the stationary reference frame denoted as d and q-axes and the rotor reference frame denoted as dr and qr-axes is shown in figure 3.2 below.

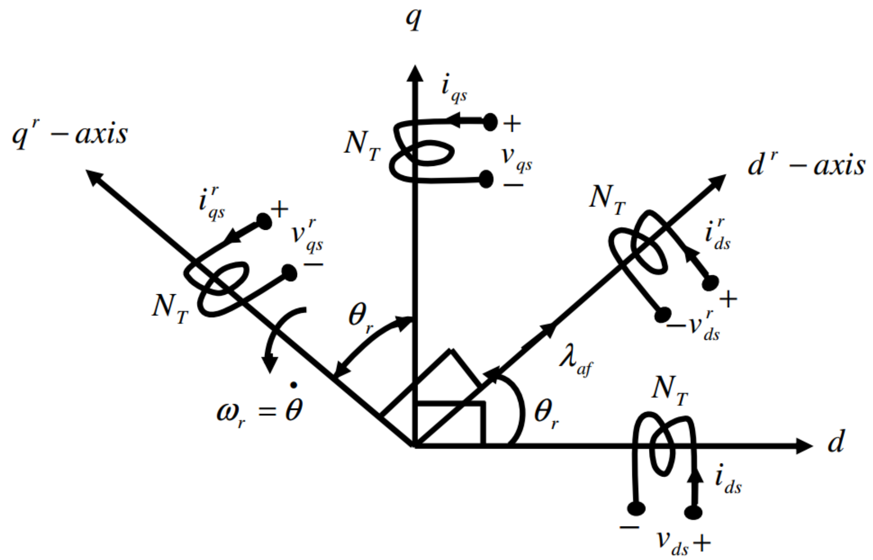

Figure 3.2: Relationship between the Stationary and Rotor Reference Frames[3]

The transformation principle is based on the fact that the fictitious stator having windings on the dr and qr-axis will produce the same mmf as the actual stator on the q and d- axis. Therefore, applying vector resolution on the figure 3.2.The relationship between the currents in the stationary reference frames i.e.,the actual winding currents and the rotor reference frames currents, i.e., the fictitious currents is written as

$$N_T i_{qs} = N_T i_{qs}^r \cos\theta_r + N_T i_{ds}^r \sin\theta_r \tag{3.17}$$

$$N_T i_{ds} = N_T i_{qs}^r \sin\theta_r + N_T i_{ds}^r \cos\theta_r \tag{3.18}$$

$$\begin{bmatrix} i_{qs} \\ i_{ds} \end{bmatrix} = \begin{bmatrix} \cos\theta_r & \sin\theta_r \\ -\sin\theta_r & \cos\theta_r \end{bmatrix} \begin{bmatrix} i_{qs}^r \\ i_{ds}^r \end{bmatrix} \tag{3.19}$$

In compact form

$$i_{qds} = [T^r] i_{qds}^r \tag{3.20}$$

where

$$i_{qds} = [i_{qs} \quad i_{ds}]^t \tag{3.21}$$

$$T^r = \begin{bmatrix} \cos\theta_r & \sin\theta_r \\ -\sin\theta_r & \cos\theta_r \end{bmatrix} \tag{3.22}$$

$$i_{qds}^r = [i_{qs}^r \quad i_{ds}^r] \tag{3.23}$$

It follows that

$$i_{qds}^r = [T^r]^{-1} i_{qds} \tag{3.24}$$

$$[T^r]^{-1} = \begin{bmatrix} \cos\theta_r & \sin\theta_r \\ -\sin\theta_r & \cos\theta_r \end{bmatrix}^{-1} = \begin{bmatrix} \cos\theta_r & -\sin\theta_r \\ \sin\theta_r & \cos\theta_r \end{bmatrix} \tag{3.25}$$

The speed of the rotor reference frame is

$$\dot{\theta}_r = \omega_r \tag{3.26}$$

Where $\dot{\theta}_r$ is the time derivative of the electrical rotor position in rad/s.

like wise, the relationship between the stationary and rotor reference frames voltages is derived as

$$V_{qds} = [T^r] V_{qds}^r \tag{3.27}$$

Where

$$V_{qds} = [V_{qr} \quad V_{ds}]^t \tag{3.28}$$

$$V_{qds}^r = [V_{qs}^r \quad V_{ds}^r]_t \tag{3.29}$$

like in the case of current,

$$V_{qds}^r = [T^r]^{-1} V_{qds} \tag{3.30}$$

Substituting equations 3.20 and 3.27 into equation 3.6 and 3.7 simplifying, the PMSM model in rotor reference frame is obtained as

$$\begin{bmatrix} V_{qs}^r \\ V_{ds}^r \end{bmatrix} = \begin{bmatrix} R_s + L_q p & \omega_r L_d \\ -\omega_r L_q & R_s + L_d p \end{bmatrix} \begin{bmatrix} i_{qs}^r \\ i_{ds}^r \end{bmatrix} + \begin{bmatrix} \omega_r \lambda_{af} \\ 0 \end{bmatrix} \tag{3.31}$$

3.2 Three Phase Permanent Magnet Synchronous Motor Model

The figure 3.3 below shows the phasor relationship between the three phase windings and the two phase dq windings.

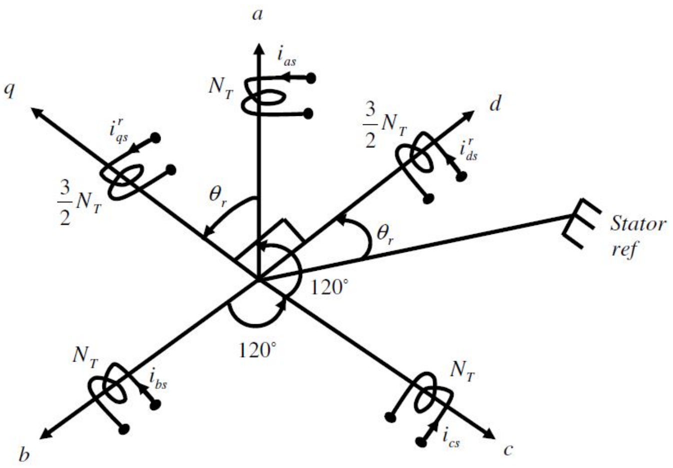

Figure 3.3: Equivalence of Three Phase and Two Phase Windings[3]

Assuming that each of the three phase windings have NT turns, then to ensure mmf equality, the two-phase windings will have 3NT/2 turns per phase. The d and q-axes mmf are found by resolving the mmfs of the three phase along the d and q-axes just as we did for the two-phase machine. The q-axis here is assumed to be lagging behind the a-axis by θ_r. The relationship between qd0 and abc currents is

$$\begin{bmatrix} i^r_q \\ i^r_d \\ i_o \end{bmatrix} = \frac{2}{3} \begin{bmatrix} \cos\theta_r & \cos(\theta_r - \frac{2\pi}{3}) & \cos(\theta_r + \frac{2\pi}{3}) \\ \sin\theta_r & \sin(\theta_r - \frac{2\pi}{3}) & \sin(\theta_r + \frac{2\pi}{3}) \\ \frac{1}{2} & \frac{1}{2} & \frac{1}{2} \end{bmatrix} \begin{bmatrix} i_{as} & i_{bs} & i_{cs} \end{bmatrix} \tag{3.32}$$

The zero sequence current i_o represents the imbalance in the abc phases. again equation 3.32 represented as

$$i^r_{qdo} = [T_{abc}]i_{abc} \tag{3.33}$$

$$i^r_{qdo} = \begin{bmatrix} i^r_{qs} & i^r_{ds} & i_o \end{bmatrix}^t \tag{3.34}$$

$$i_{abc} = \begin{bmatrix} i_{as} & i_{bs} & i_{cs} \end{bmatrix}^t \tag{3.35}$$

and the transformation from abc to qdo variables is

$$[T_{abc}] = \frac{2}{3}\begin{bmatrix} \cos\theta_r & \cos(\theta_r - \frac{2\pi}{3}) & \cos(\theta_r + \frac{2\pi}{3}) \\ \sin\theta_r & \sin(\theta_r - \frac{2\pi}{3}) & \sin(\theta_r + \frac{2\pi}{3}) \\ \frac{1}{2} & \frac{1}{2} & \frac{1}{2} \end{bmatrix} \tag{3.36}$$

The zero sequence current,i_o does not produce a resultant magnetic filed.The transformation from the two-phase stator currents can be obtained as

$$i_{abc} = [T_{abc}]^{-1} i^r_{qdo} \tag{3.37}$$

where

$$[T_{abc}]^{-1} = \begin{bmatrix} \cos\theta_r & \sin\theta_r & 1 \\ \cos(\theta_r - \frac{2\pi}{3}) & \sin(\theta_r - \frac{2\pi}{3}) & 1 \\ \cos(\theta_r + \frac{2\pi}{3}) & \sin(\theta_r + \frac{2\pi}{3}) & 1 \end{bmatrix} \tag{3.38}$$

For a balanced system,$i_a + i_b + i_c = 0$. It is important to note that for unbalanced system,$i_a + i_b + i_c \neq 0$. For such an unbalanced system, the zero sequence term is written as:

$$v_o = R_s i_o + p\lambda_o = R_s + L_o p i_o \tag{3.39}$$

where

λ_o is the zero sequence flux linkages

L_o is the zero sequence inductance

i_o is the zero sequence current

The PMSM model for a three phase unbalanced system is

$$\begin{bmatrix} v^r_{qs} \\ v^r_{ds} \\ v_o \end{bmatrix} = \begin{bmatrix} R_s + L_q p & \omega_r L_d & 0 \\ -\omega_r L_q & R_s + L_d p & 0 \\ 0 & 0 & R_s + L_o p \end{bmatrix} \begin{bmatrix} i^r_{qs} \\ i^r_{ds} \\ i_o \end{bmatrix} + \begin{bmatrix} \omega_r \lambda_{af} \\ 0 \\ 0 \end{bmatrix} \tag{3.40}$$

But, for a balanced system, where.PMSM model in rotor reference frame $i_a + i_b + i_c = 0$ remains

$$\begin{bmatrix} V^r_{qs} \\ V^r_{ds} \end{bmatrix} = \begin{bmatrix} R_s + L_q p & \omega_r L_d \\ -\omega_r L_q & R_s + L_d p \end{bmatrix} \begin{bmatrix} i^r_{qs} \\ i^r_{ds} \end{bmatrix} + \begin{bmatrix} \omega_r \lambda_{af} \\ 0 \end{bmatrix} \tag{3.41}$$

3.2.1 Development of the PMSM Power and Torque Relationships

The power input to the three-phase machine has to the power input to the two-phase machine to have meaningful interpretation in the modeling,analysis,and simulation and Electromagnetic torque is the most important output variable that determines the mechanical dynamics of the machine such as the rotor position and speed. It is derived from the machine matrix equation by looking at the input power and its various components such as resistive loss component, mechanical power and the rate of change of stored magnetic energy.

The three-phase instantaneous power input is

$$P_i = v_{abc}^t i_{abc} = \begin{bmatrix} v_{as} & v_{bs} & v_{cs} \end{bmatrix} \begin{bmatrix} i_{as} \\ i_{bs} \\ i_{cs} \end{bmatrix} = v_{as}i_{as} + v_{bs}i_{bs} + v_{cs}i_{cs} \tag{3.42}$$

From Equation 3.33 and 3.37

$$i_{abc} = [T_{abc}]^{-1} i_{qdo}^r \tag{3.43}$$

$$v_{abc} = [T_{abc}]^{-1} v_{qdo}^r \tag{3.44}$$

Substituting Equation 3.43 and 3.44 in to Equation 3.42

$$P_i = \frac{3}{2}[(v_{qs}^r i_{qs}^r + v_{ds}^r i_{ds}^r) - 2v_o i_o] \tag{3.45}$$

For a balanced system, the zero sequence current i_o does not exist.hence

$$P_i = \frac{3}{2}[v_{qs}^r i_{qs}^r + v_{ds}^r i_{ds}^r] \tag{3.46}$$

From equation 3.41, the dynamic equation of the PMSM can be written as

$$V = [R]i + [L]pi + [G]\omega_r i \tag{3.47}$$

Where:

[R] matrix consist of resistive elements

[L] matrix consists of the derivatives of the operator p

[G] matrix has elements that are the coefficients of the electrical speed ω_r.

Multiplying both sides of equation 4.47 with the transpose of the vector current

$$P_i = i^t V = i^t[R]i + i^t[L]pi + i^t[G]\omega_r i \tag{3.48}$$

Where:

$i^t[R]i$ is stator and rotor resistive losses

$i^t[L]pi$ is the rate of change of stored magnetic energy.This is zero at steady state.

$i^t[G]\omega_r i$ is the mechanical power

From the fundamentals ,it is known that the air gap torque has to be associated with the rotor speed.The air gap power is the product of the mechanical rotor speed and air gap or electromagnetic torque that is

$$\omega_m T_e = P_a = i^t[G]i \times \omega_r = i^t[G]i\frac{p}{2}\omega_m \tag{3.49}$$

where p is the number of pole.dividing both side by ω_m leads to an electromagnetic torque i.e.,

$$T_e = \frac{p}{2}i^t[G]i \tag{3.50}$$

Substituting for G in equation 3.50, the electromagnetic torque is obtained as

$$T_e = \frac{3}{2}\frac{p}{2}[\lambda_{af} + (L_q - L_d)i^r_{ds}]i^r_{qs} \qquad (N.m) \tag{3.51}$$

When $Lq = L_d$ i.e.,for Surface mounted PMSM the electromagnetic torque is obtained as

$$T_e = \frac{3}{2}\frac{p}{2}[\lambda_{af} i^r_{qs}] \qquad (N.m) \tag{3.52}$$

Here we can formulate our input power interms of rotor reference stator current and voltage that is

$$P_i = \frac{3}{2}[v^r_{qs}i^r_{qs} + v^r_{ds}i^r_{ds}] \tag{3.53}$$

3.2.2 Steady State Torque Characteristics

It is important to examine the steady state torque characteristics of the motor to highlight the relationship between the torque angle and the various torque components. Assume the following set of balanced polyphase current as the input to the stator of a salient pole PMSM:

$$I_{qs} = I_m \sin(\omega_r t + \delta) \tag{3.54}$$

$$I_{ds} = I_m \cos(\omega_r t + \delta) \tag{3.55}$$

δ is the angle between the rotor field flux λ_{af} and stator current phasor and known as the torque angle since it determines the steady state torque. Using the inverse transformation ratio $[T^t]^{-1}$

$$[T^t]^{-1} = \begin{bmatrix} \cos\theta_r & -\sin\theta_r \\ \sin\theta_r & \cos\theta_r \end{bmatrix} \tag{3.56}$$

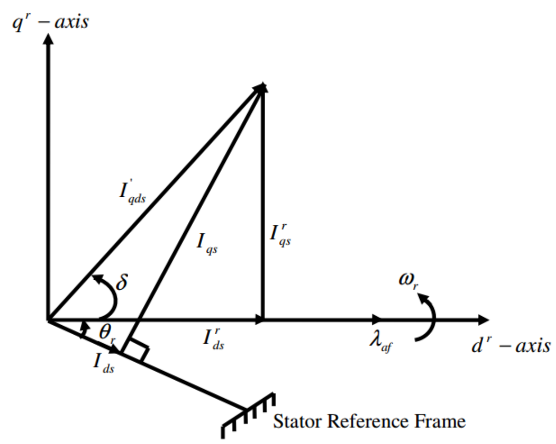

Figure 3.4: Stator Input Current Phasor Diagram[3]

The steady state stator current components in the rotor reference frame as shown in figure 3.4 are

$$I^r_{qs} = I_m \sin\delta \tag{3.57}$$

$$I^r_{ds} = I_m \cos\delta \tag{3.58}$$

And substituting these into the torque expression(i.e., in Equation 3.51),the air gap torque is obtained as

$$T_e = \frac{3}{2}\frac{p}{2}[\lambda_{af} I_m \sin\delta + \frac{1}{2}(L_d - L_q) I_m^2 \sin 2\delta] \tag{3.59}$$

The torque angle δ directly influences the airgap torque T_e . The torque expression contains two components; the synchronous torque T_{es} (excitation torque) which is due to the interaction of the rotor magnetic field and the q axis stator current and the reluctance torque T_{er} due to reluctance variation.

They are related as:

$$T_{es} = \frac{3}{2}\frac{p}{2}\lambda_{af} I_m \sin\delta \tag{3.60}$$

$$T_{er} = \frac{3}{2}\frac{p}{2}[\frac{1}{2}(L_d - L_q)] I_m^2 \sin 2\delta \tag{3.61}$$

$$T_e = T_{es} + T_{er} \tag{3.62}$$

3.2.3 Equivalent Circuit Representation of PMSM

The dynamic equation of the PMSM in rotor reference frames can be represented using flux linkages as a variables.

$$\lambda_{qs}^r = L_q i_{qs}^r \tag{3.63}$$

$$\lambda_{ds}^r = L_d i_{ds}^r + \lambda_{af} \tag{3.64}$$

From the above Equations,the stator currents in the rotor reference frames can be represented in terms of flux linkages and inductance.
Then the q and d axis stator voltages in terms of these flux linkages in the rotor reference frames as follows:

$$v_{qs}^r = R_s i_{qs}^r + p\lambda_{qs}^r + \omega_r \lambda_{ds}^r \tag{3.65}$$

$$v_{ds}^r = R_s i_{ds}^r + p\lambda_{ds}^r - \omega_r \lambda_{qs}^r \tag{3.66}$$

Flux linkage are defined as follows:

$$\lambda_{qs}^r = L_q i_{qs}^r \tag{3.67}$$

$$\lambda_{ds}^r = L_d i_{ds}^r + \lambda_{af}^r \tag{3.68}$$

The airgap torque is also obtained in terms of the flux linkages by substituting equations 3.63 and 3.64 into equation 3.51 as shown below

$$T_e = \frac{3}{2}\frac{p}{2}\frac{1}{L_q}[\rho\lambda_{af} + (1-\rho)\lambda_{ds}^r]\lambda_{qs}^r \tag{3.69}$$

$$T_e = \frac{3}{2}\frac{p}{2}[\lambda_{ds}^r i_{qs}^r - \lambda_{qs}^r i_{ds}^r] \tag{3.70}$$

where the saliency ratio is defined as

$$\rho = \frac{L_q}{L_d} \tag{3.71}$$

Since surface mounted PMSM $L_q = L_d$ therefore $\rho = 1$.

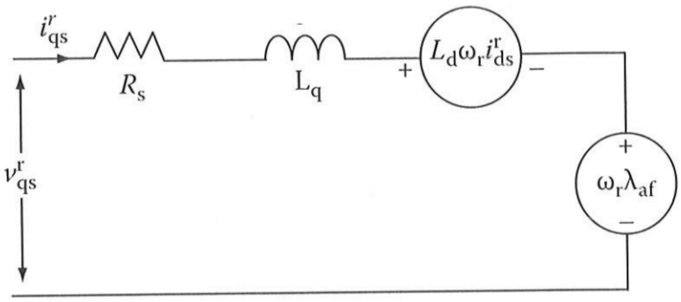

(a) q-axis equivalent circuit

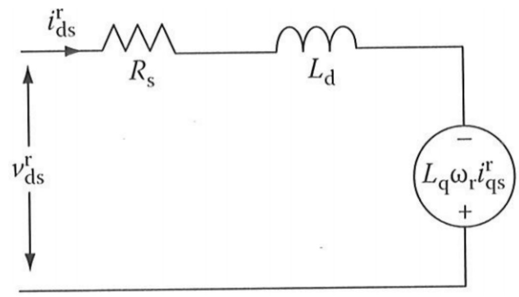

(b) d-axis equivalent circuit

Figure 3.5: d-q equivalent circuit in synchronously rotating frame [3]

3.3 Vector Control of PMSM

Vector control, by field orientation, is used to decouple the stator current of the PMSM into equivalent flux and torque producing current components for independent and precise control of torque and flux like in DC machine as shown in the phasor diagram of Fig. 3.6. The resolution of the stator current phasor on the rotating direct and quadrature axes (known as rotor reference frames) gives i^r_{ds} and i^r_{qs}, respectively.and they related as:

$$\begin{bmatrix} i^r_{qs} \\ i^r_{ds} \end{bmatrix} = i_s \begin{bmatrix} \sin\delta \\ \cos\delta \end{bmatrix} \tag{3.72}$$

Note that they are constants for agiven stator current phasor and torque angle. The stator current component along the rotor flux axis,i.e, along rotating d-axis, can only produce a flux and hence can be named as the flux-producing component of stator current and denoted as i_f.This current only partially contributes to the d-axis and the remaining part of the rotor flux is contributed by the PMs.The component that is in quadrature to the rotor flux can produce a torque in interaction withe the rotor flux and hence named as torque-producing current.i_T very similar to the armature current of the separately excited dc motor.

$$i_{qs}^r = i_T \tag{3.73}$$

$$i_{ds}^r = i_f \tag{3.74}$$

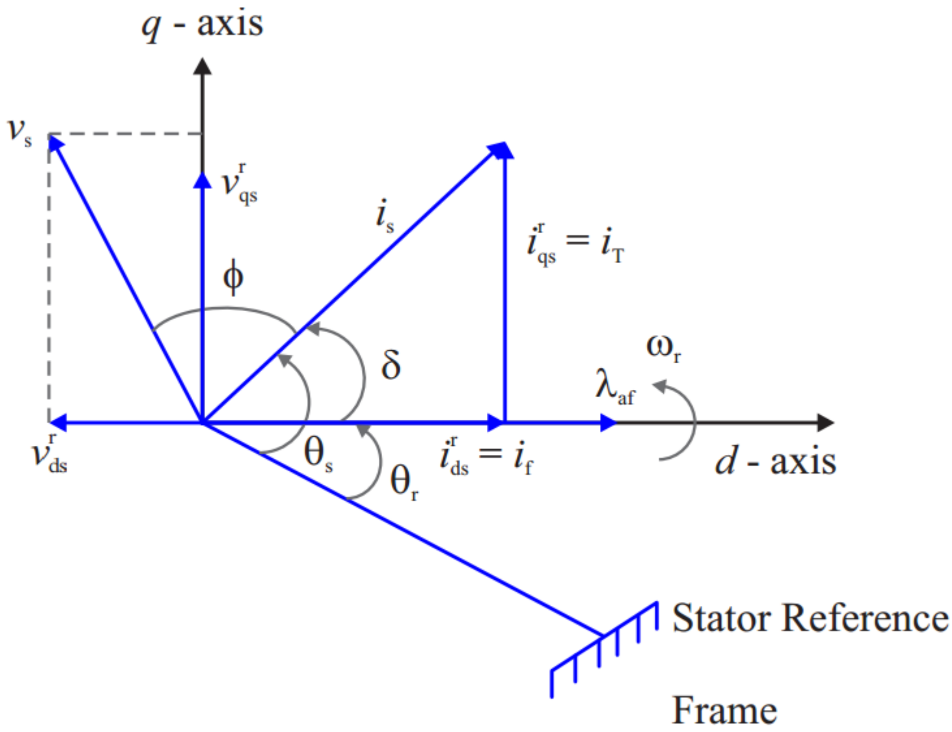

Figure 3.6: Phasor diagram of vector control by FOC for PMSM

As shown in Fig. 3.6, the rotor flux linkage revolves at a rotor speed ω_r and is positioned away from a stationary reference by the rotor angle θ_r . The stator current phasor is at angle δ from the rotor flux linkages phasor. Field orientation control is achieved by making $\delta = 90^o$ thereby making the stator flux current component zero.

$$i_f = i_{ds}^r = i_s \cos\delta = 0 \tag{3.75}$$

Therefore,

$$T_e = \frac{3}{2}\frac{p}{2}\lambda_{af} i_s = K_t i_s \tag{3.76}$$

where $K_t = \frac{3}{2}\frac{p}{2}\lambda_{af}$ is the torque constant. Under this condition, the PMSM behaves exactly as the separately excited dc motor [8] as seen from the torque expression where the torque is produced by the interaction of the rotor flux and the stator current.

3.4 Per Unit Model

The normalizing model of the PMSM is derived by defining the base variables both in the abc and dqo variables.in the abc frame, let the rms value of rated phase voltages and currents in abc frame result in

$$Basepower = P_b = 3V_{b3}I_{b3} \tag{3.77}$$

Where v_{b3} and I_{b3} are the three-phase voltage and current, respectively.Selecting the base quantities in the dq frames denoted by V_b and I_b to be equal to the peak value of the phase voltage and current in abc frames result in

$$V_b = \sqrt{2}V_{b3} \tag{3.78}$$

$$I_b = \sqrt{2}I_{b3} \tag{3.79}$$

Therefor,the base power is defined as

$$P_b = 3V_{b3}I_{b3} = 3\frac{V_b}{\sqrt{2}}\frac{I_b}{\sqrt{2}} = \frac{3}{2}V_bI_b \tag{3.80}$$

The rotor reference frame model begin with considering the q-axis stator voltage,which is given in the following:

$$v_{qs}^r = (R_s + L_qP)i_{qs}^r + \omega_r(L_di_{ds}^r + \lambda_{af}) \tag{3.81}$$

It is normalized by dividing it with the base voltage,V_b as

$$v_{qsn}^r = \frac{v_{qs}^r}{V_b} = \frac{R_s}{V_b}i_{qs}^r + \frac{L_q}{V_b}pi_{qs}^r + \frac{\omega_r(L_qi_{ds}^r + \lambda_{af})}{V_b}(p.u) \tag{3.82}$$

Base voltage in terms of base current, I_b , and base impedance ,Z_b or base speed and base flux linkage as

$$V_b = I_bZ_b = \omega_b\lambda_b = \omega_bL_bI_b \quad (V) \tag{3.83}$$

Substituting V_b in to Equation 3.80 yields

$$v_{qs}^r = (\frac{R_s}{Z_b})(\frac{i_{qs}^r}{I_b}) + \frac{1}{\omega_b}(\frac{L_q}{L_b})p(\frac{i_{dr}^r}{I_b}) + (\frac{\omega_r}{\omega_b})[(\frac{L_d}{L_b})(\frac{i_{ds}^r}{I_b}) + \frac{\lambda_{af}}{\lambda_b}] \quad (p.u) \tag{3.84}$$

Defining the normalized parameters and variables in the following manner:

$$R_{sn} = \frac{R_s}{Z_b}(p.u), \quad L_{qn} = \frac{L_q}{L_b}(p.u), \quad L_{dn} = \frac{L_d}{L_b}(p.u), \quad \omega_{rn} = \frac{\omega_r}{\omega_b}(p.u) \tag{3.85}$$

$$i^r_{qsn} = \frac{i^r_{qs}}{I_b}(p.u), \quad i^r_{dsn} = \frac{i^r_{ds}}{I_b}(p.u), \quad v^r_{qsn} = \frac{v^r_{qs}}{V_b}(p.u), \quad v^r_{dsn} = \frac{v^r_{ds}}{V_b}(p.u)$$

Similarly, the d-axis stator voltage equation is normalized

$$v^r_{dsn} = -\omega_{en} L_{qn} i^r_{dsn} + (R_{sn} + \frac{L_{dn}}{\omega_b} p) i^r_{dsn} \quad (p.u) \tag{3.86}$$

$$T_b = \frac{P_b}{\frac{\omega_b}{P/2}} = \frac{P}{2}\frac{P_b}{\omega_b} = \frac{P}{2}\frac{3}{2}\frac{V_b I_b}{\omega_b} = \frac{3}{2}\frac{P}{2}\lambda_b I_b \quad (N.m) \tag{3.87}$$

From which the normalized electromagnetic torque(for surface mounted PMSM) is obtained as

$$T_{en} = \frac{T_e}{T_b} = i^r_{qsn}\lambda_{afn} \quad (p.u) \tag{3.88}$$

Where

$$\lambda_{afn} = \frac{\lambda_{af}}{\lambda_b} \quad (p.u) \tag{3.89}$$

The electromechanical dynamic equation is given by

$$T_e = J\frac{d\omega_m}{dt} + T_l + B\omega_m \tag{3.90}$$

Where

ω_m is the mechanical rotor speed

J is the moment of inertia of the load and machine combined

B is the friction coefficient of the load and the machine,

T_l is the load torque

3.5 Pulse Width Modulation

The control of harmonics and variation of the fundamental component can be achieved by varying the duration of applied input voltage to the machine.It is realized by changing the pulse width to gate signals of the inverter and it is known as PWM schemes,In general aim to maximize the fundamental harmonics. Figure 3.7 shows sample wave form of phase a and its mid point voltage for the inverter given in Figure 3.8 .The intersection of carrier signal v_c(abidirectional triangular wave form) provide the switching signals to the base drive of the inverter switches.The switching logic for one phase is given as:

$$v_{an} = \frac{1}{2}V_{dc}, \qquad v_c < v_a^* \tag{3.91}$$
$$v_{an} = -\frac{1}{2}V_{dc}, \qquad v_c > v_a^*$$

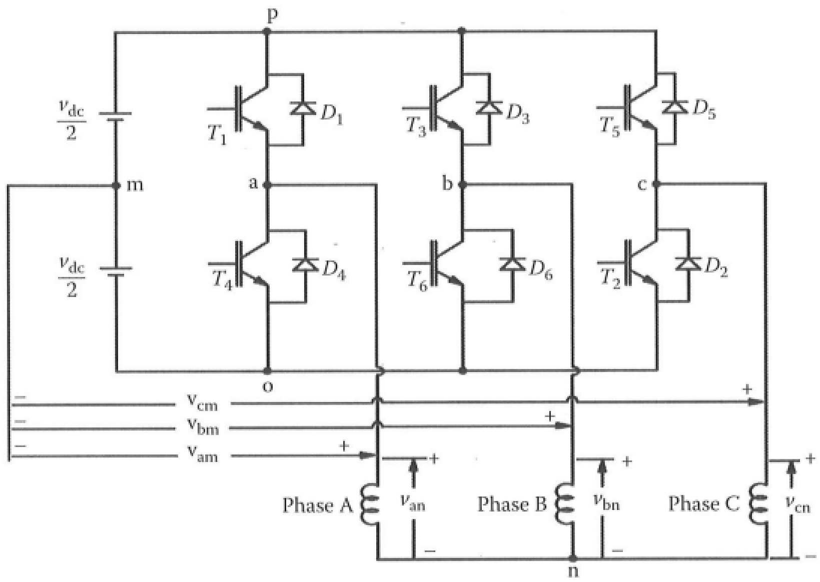

Figure 3.7: Three-phase inverter[3]

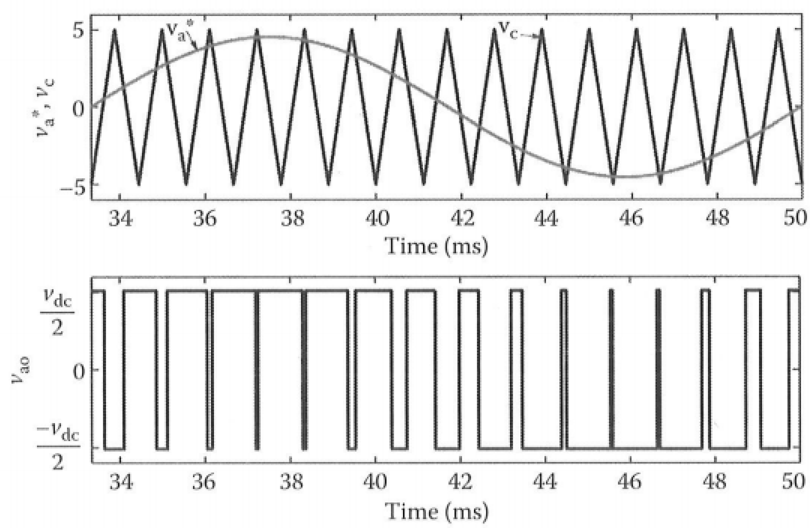

Figure 3.8: Sinsoidal PWM[3]

The fundamental of this midpoint voltage is

$$v_{am1} = \frac{V_{dc}}{2}\frac{v_a^*}{v_{cp}} \tag{3.92}$$

where

v_a^* is the peak value of the phase reference or command signal

v_{cp} is the peak value of the triangular carrier signal

The resulting output follows the frequency and phase of the reference signal.The modulation index or ratio is defined by

$$m = \frac{v_a^*}{v_{cp}} \tag{3.93}$$

which substituted in Equation 3.92 gives

$$v_{am1} = m\frac{V_{dc}}{2} \tag{3.94}$$

The line to line rms voltage is derived from the mid point voltage v_{am1} as

$$V_\ell = \frac{\sqrt{3}}{\sqrt{2}}v_{am1} \tag{3.95}$$

where

m is the modulation ratio

V_{dc} is the dc link voltage or input voltage to the inverter

The modulation ratio from Equation 3.93 can be written as

$$m = \frac{(\frac{\sqrt{3}}{\sqrt{2}}V_\ell)}{(\frac{V_{dc}}{2})} = \frac{\sqrt{2}V_{ph}}{(\frac{V_{dc}}{2})} = \frac{V_p}{(\frac{V_{dc}}{2})} \tag{3.96}$$

where V_p is the peak phase voltage.From this equation ,it is seen that the modulation ratio between fundamental peak phase voltage and the midpont voltage with respect to dc source midpoint input.It is seen by this definition that the mpdulation ratio is normalized with respect to mid point of dc source input.The line to line voltage output is linear for the modulation ratio from zero to one.Beyond that range,the out put voltage increases but not linearly and it is known as over modulation region.This region from this value to maximum line to line voltage is divided into two sub regions.In the subregion where the modulation ratio is between 1 and 1.154,and the line to line rms voltage at m=1.154 is derived as[4].

$$V_\ell = \frac{\sqrt{3}}{\sqrt{2}} m \frac{V_{dc}}{2} = \frac{\sqrt{3}}{2}(1.154\frac{V_{dc}}{2}) = 0.707V_{dc} \tag{3.97}$$

and it corresponds to a peak phase voltage given by

$$V_{am1} = \frac{2}{3}V_{dc}\sin 60^o = \frac{V_{dc}}{\sqrt{3}} = 0.577V_{dc} \tag{3.98}$$

CHAPTER 4:

FIELD WEAKENING TECHNIQUE FOR PMSM

Due to the upper limit placed on the available dc link voltage and current ratings of a given inverter, the motor input voltage and current ratings are limited. The voltage and current rating are limits impact the maximum speed with rated torque capability and the maximum torque producing capability of the motor drive system, respectively. It is required and desirable to produce the rated power with the highest attainable speed for many applications such as electric vehicles, people carriers in airport lobbies, forklifts, machine tool spindle drives, etc. corresponding to the maximum dc link voltage and hence the maximum input machine attains a speed known as the rated (base) speed. Above this speed, the induced emf will exceed the maximum input voltage, making the flow of current into machine phases impractical. To overcome this situation, the induced emf is constrained to be less than the applied voltage by weakening the air gap flux linkages. The flux weakening is made to be inversely proportional to the stator frequency so that the induced emf is a constant and will not increase with the increasing speed.

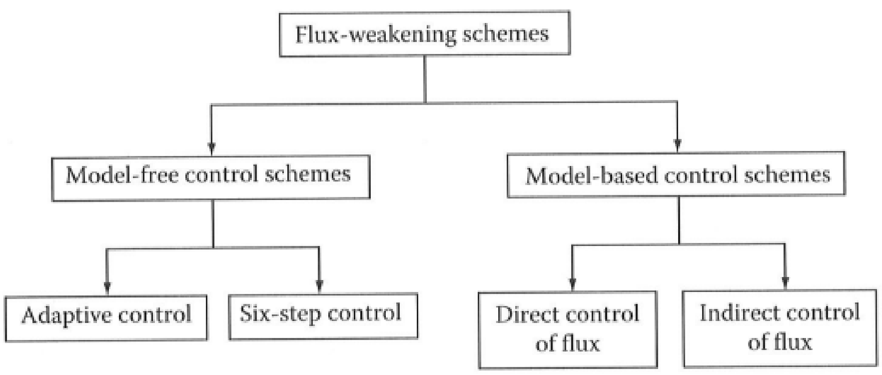

Figure 4.1: classification of flux-weakening control schemes

4.1 Indirect Control Scheme

The scheme does not request a specific air gap flux request directly in its controller but implements the flux weakening in an indirect manner. It is achieved by only considering the rotor speed request, and accordingly the d-axis current for that speed is computed. This, together with the stator q-axis current that is allowed within the maximum allowable stator current magnitude, determines the torque generation and indirectly the air gap flux. Schematically the control scheme is shown in figure 4.2. Assuming a speed controlled drive system, the torque command T_{ec}, is generated by the speed error. Depending on the mode of operation, the torque command is processed by block 1 or 2. Block 1 corresponds to the constant torque mode controller whereas block 2 corresponds to the flux-weakening mode controller. The outputs of the controllers are stator current magnitude command and the torque angle command. They, together with the electrical rotor position, provide the phase current commands through the stator reference transformation block. Then the resulting stator current commands in stator reference frames are enforced with an inverter by current feedback control, with any one of the current control schemes available. The rotor position and the rotor speed are assumed to be obtained with an encoder and a signal conditioner, respectively. induced emf is a constant and will not increase with the increasing speed.

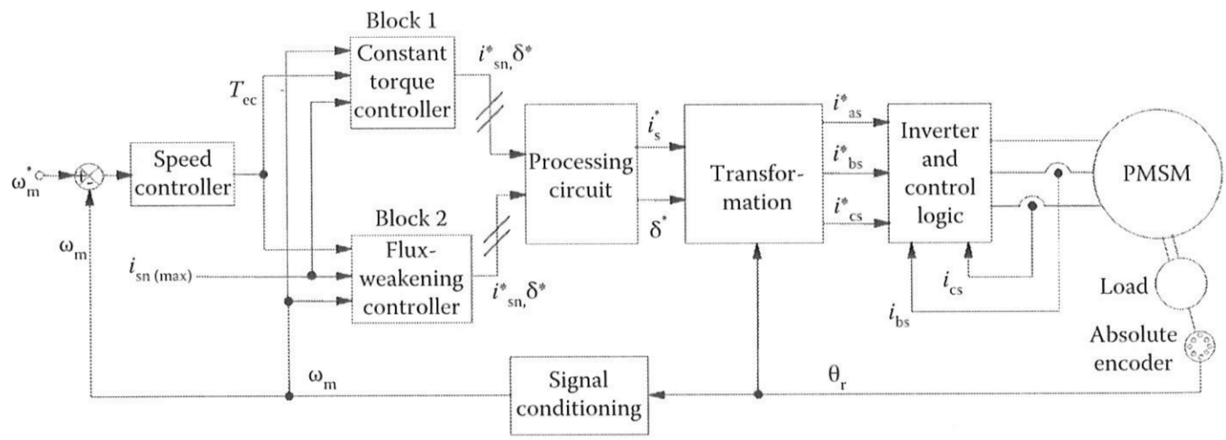

Figure 4.2: Schematic of the PMSM Control Strategy [3]

4.2 Maximum Speed

To understand the scope of the flux weakening of the pmsm drive,it is essential to detererrmine the maximum speed.The maximum speed for a given set of stator voltages and currents is obtained analytically for the purpose of design calculations. The maximum operating speed with zero torque is calculated from the steady state stator voltage equation as follows.The normalized stator voltage equations in the rotor reference frames are given as

$$v^r_{qsn} = (R_{sn} + L_{qnp})i^r_{qsn} + \omega_{rn}(L_{dsn}i^r_{dsn} + 1) \tag{4.1}$$

$$v^r_{dsn} = -\omega_{rn}L_{qn}i^r_{qsn} + (R_{sn} + L_{dn}p)i^r_{dsn} \tag{4.2}$$

where the abc to dq transformation valid for voltages,currents,and flux linkage is used to obtain the voltages in rotor reference frames as.

$$\begin{bmatrix} v^r_{qsn} \\ v^r_{dsn} \end{bmatrix} = \frac{2}{3}\begin{bmatrix} \cos\theta_r & \cos(\theta_r - \frac{2\pi}{3}) & \cos(\theta_r - \frac{2\pi}{3}) \\ \sin\theta_r & \sin(\theta_r - \frac{2\pi}{3}) & \sin(\theta_r - \frac{2\pi}{3}) \end{bmatrix}\begin{bmatrix} V_{an} \\ V_{bn} \\ V_{cn} \end{bmatrix} \tag{4.3}$$

The steady state stator voltage equations are obtained by putting the derivative of the current variable to zero in Equation 4.1 as

$$v^r_{qsn} = R_{sn}i^r_{qsn} + \omega_{rn}(L_{dsn}i^r_{dsn} + 1) \tag{4.4}$$

$$v^r_{dsn} = -\omega_{rn}L_{qn}i^r_{qsn} + R_{sn}i^r_{dsn} \tag{4.5}$$

The maximum speed is attained by letting the air gap flux reduce drastically and all the stator current is utilized for that purpose only.That means the q axis current is zero,i.e., i^r_{qsn}=0.The stator voltage phasor then obtained as

$$v^2_{sn} = (v^r_{dsn})^2 + (v^r_{qsn})^2 = \omega^2_{rn}(1 + L_{dn}i^r_{dsn})^2 + R^2_{sn}(i^r_{dsn})^2 \tag{4.6}$$

From which the maximum speed for a given stator current magnitude of i^r_{dsn} is

$$\omega_{rn}(max) = \frac{\sqrt{v^2_{sn} - R^2_{sn}(i^r_{dsn})^2}}{(1 + L_{dn}i^r_{dsn})} \tag{4.7}$$

4.3 Flux-Weakening Algorithm

Consdering steady state and by neglecting the resistive terms, the voltage phasor is written as

$$v_{sn}^2 = \omega_{rn}^2(1 + L_{dn}i_{dsn}^r)^2 + (L_{qn}i_{qsn}^r)^2 \quad (p.u) \tag{4.8}$$

Where the voltage phasor ,v_{sn} is defined as

$$v_{sn} = \sqrt{(v_{qsn}^r)^2 + (v_{dsn}^r)^2} \quad (p.u) \tag{4.9}$$

The quadrature current i_{qsn}^r can be written in terms of the stator current phasor and stator direct-axis current as

$$i_{qsn}^r = \sqrt{(i_{sn}^r)^2 - (i_{dsn}^r)^2} \tag{4.10}$$

4.4 Voltage and current limits

First, consider the current ratings of the inverter switches at maximum allowed machine stator current I_{max}. The maximum allowed current can then be represented in the synchronously rotating frame iq-id plane as a circle centered at the origin and with radius I_{max}. Normalizing the maximum current to unity, the circle is then centered at zero with radius 1.The interior of this circle represents the locus where current regulators can generate any normalized current phasor without exceeding the current limits of the drive system. Figure 4.3 shows the current limit as well as a typical armature current phasor I operating within this limit.

The other operation limit that must be considered is the maximum output voltage provided by the inverter. The output voltage of the inverter is a function of the DC link voltage. In VC, the ability to control the stator current is critical. This ability to control the current is given by the PWM operation of the inverter, and it is lost if the inverter switches saturate. Therefore, the inverter must operate within the so-called undermodulation region of the PWM.

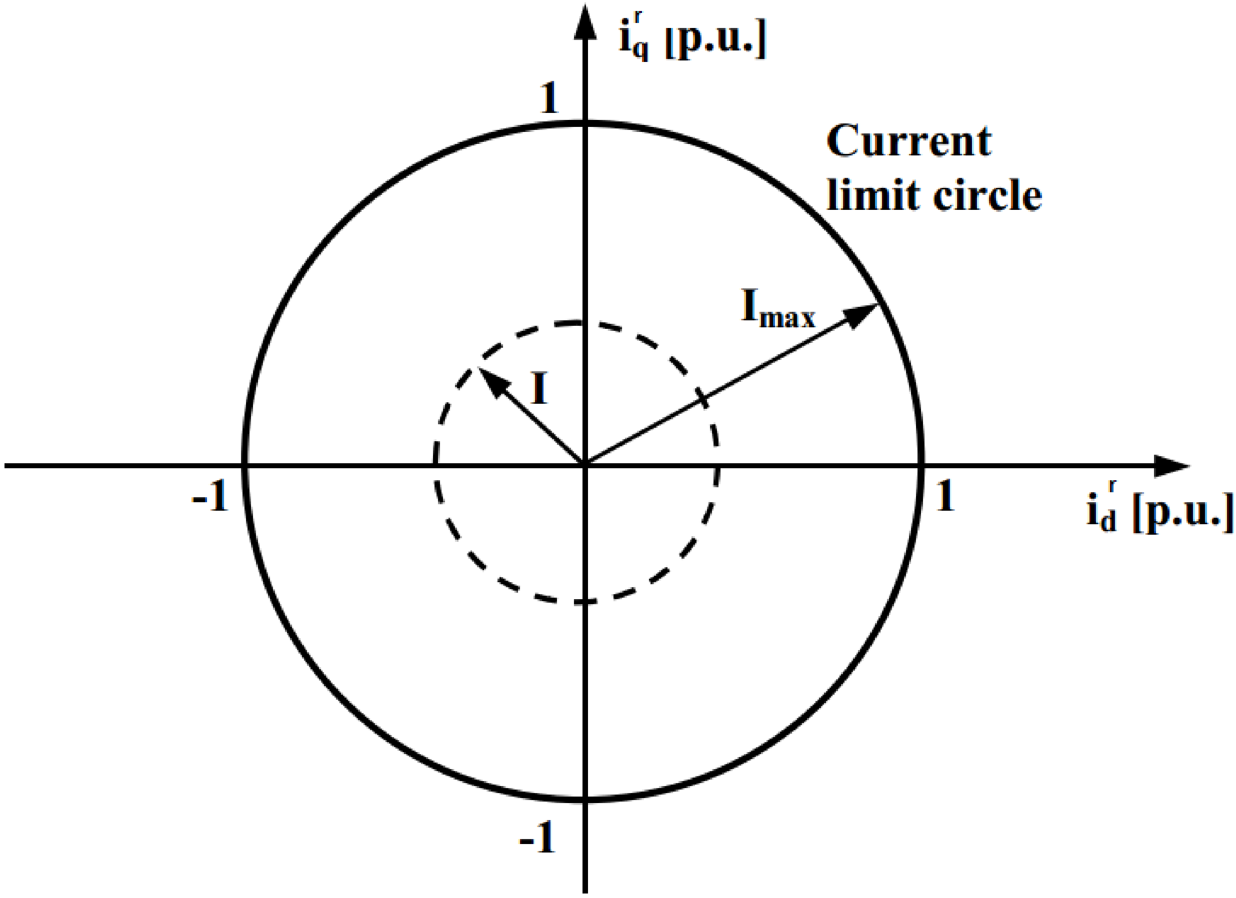

Figure 4.3: Normalized current limit circle in the synchronously rotating reference frame[36]

The condition for current constraint obtained as

$$\sqrt{(i^r_{qsn})^2 + (i^r_{dsn})^2} \leq I_{max} \tag{4.11}$$

For VC(Vector Control) of PMSM, the maximum peak value of the inverter output voltage as function of the DC link voltage is:

$$V_{max} = \frac{\sqrt{3}V_{dc}}{3} \tag{4.12}$$

The voltage constraint can also be written in the (id - iq) plane. To make the working easier, assume a non-salient machine and neglect stator resistance i.e, $L = L_d = L_q and R = 0$

$$v^r_{qsn} = i^r_{qsn}R_{sn} + \omega_{rn}L^r_{dsn}i^r_{dsn} + \omega_{rn}\lambda_{afn} \tag{4.13}$$

$$v^r_{qsn} = \omega_{rn}L^r_{dsn}i^r_{dsn} + \omega_{rn}\lambda_{afn} \tag{4.14}$$

$$v^r_{qsn} = \omega_{rn}(L^r_{dsn}i^r_{dsn} + \lambda_{afn}) = \omega_{rn}\lambda^r_{dsn} \tag{4.15}$$

$$v^r_{dsn} = i^r_{dsn}R_{sn} - \omega_{rn}L_{qsn}i^r_{qsn} \tag{4.16}$$

$$v^r_{dsn} = -\omega_{rn}L_{qsn}i^r_{qsn} = -\omega_{rn}\lambda^r_{qsn} \tag{4.17}$$

From Equation (4.9) we can obtained current constraint as:

$$v^2_{sn} = (\omega_{rn}L^r_{dsn}i^r_{dsn} + \omega_{rn}\lambda_{afn})^2 + (\omega_{rn}L_{qsn})^2(i^r_{qsn})^2 \tag{4.18}$$

$$(\frac{v_{sn}}{\omega_{rn}L_{qsn}}) = (i^r_{dsn} + \frac{\lambda_{afn}}{L_{qsn}})^2 + (i^r_{qsn})^2 \tag{4.19}$$

Equation (4.19) is equation of a circle with center is offset at $i^r_{dsn} = \frac{\lambda_{afn}}{L_{qsn}}$ and radius of $(\frac{v_{sn}}{\omega_{rn}L_{qsn}})^2$ The operation limit established by the DC link voltage can be determined by substituting the applied armature voltage v_{sn} in equation 4.18 by maximum peak value of the inverter output voltage from equation 4.12. This limit is given by:

$$(\frac{\sqrt{3}v_{dc}}{3v_b\omega_{rn}L_{qsn}}) = (i^r_{dsn} + \frac{\lambda_{afn}}{L_{qsn}})^2 + (i^r_{qsn})^2 \tag{4.20}$$

Equation 4.16 represents the family of circles that limit the operation of the PMSM due to the DC link voltage constraint. In other words, for each speed there will be a voltage limit circle. Notice that as the speed increases, the circle shrinks. Figure 4.4 shows three examples of the voltage circle limit for speeds ω_{r1}, ω_{r2}, andω_{r3}. Where ω_{r3} is bigger than ω_{r2} and ω_{r2} is bigger than ω_{r1}.

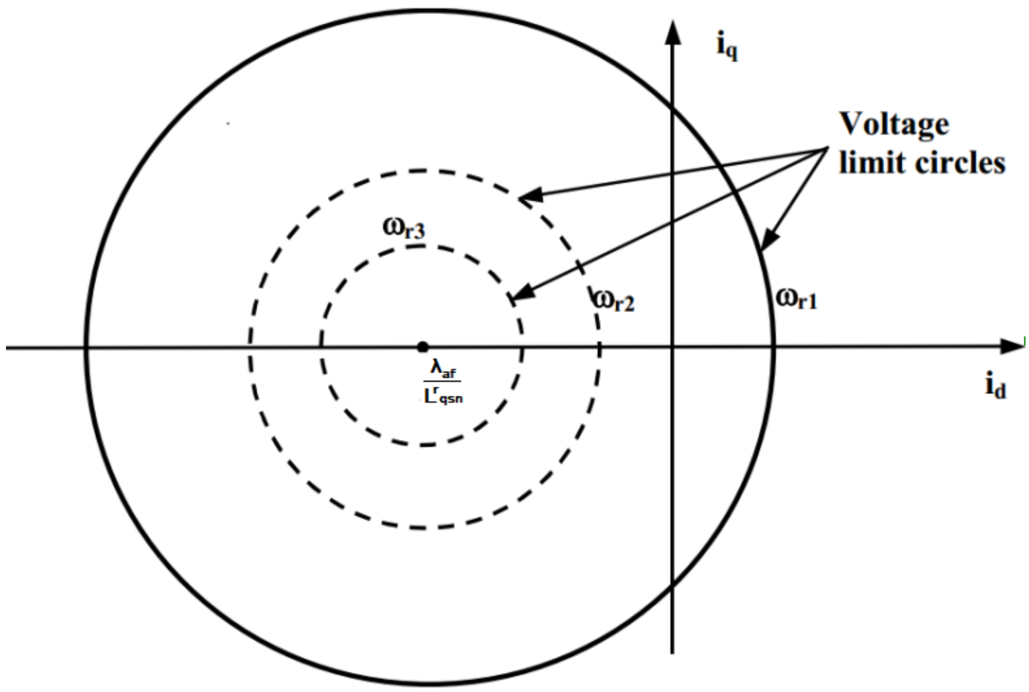

Figure 4.4: Voltage limit circles in the synchronously rotating reference frame[36]

The two constraints discussed above must be combined in order to define the drive operation limits. Notice that since the two constraints must be satisfied, the drive operation limit will then be defined by the intersection of the two circles defined by the current and voltage limits.

Figure 4.4 shows the two constraints for PMSM drive system. The current limit circle and the voltage limit circle are given. In this figure, the shaded area represents the operation region where the machine can operate at speed ω_{r2}, i. e., any armature current vector can be generated by the controller within this area and therefore any torque/speed associated with this current can be provided. The voltage limit circle in continuous line is the voltage limit circle for base speed ($\omega_{r1} = \omega_{rb}$).

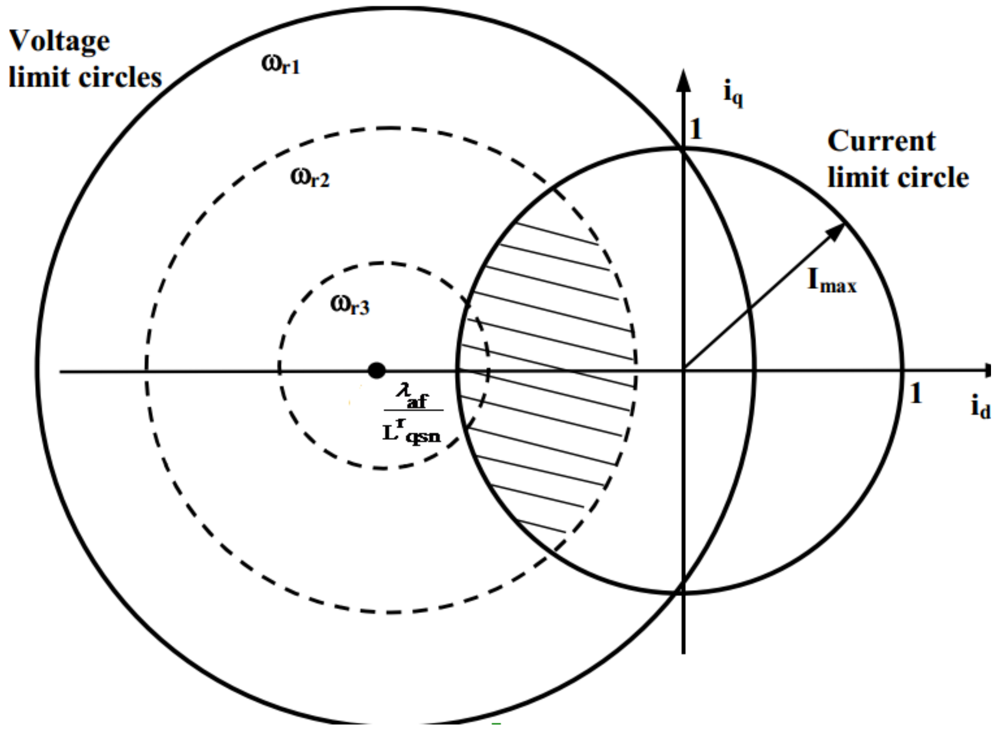

Figure 4.5: Current circle limit and voltage limit circle for PMSM drive system[36]

In order to understand the operation of VC of PMSM drive system and its operation limits, the analysis will be divided into two parts, the constant torque region and the constant power region. Analysis of the best armature current vector trajectory will also be given.

4.5 Constant Torque Operation Region

In a PMSM, the magnetic field is provided by the permanent magnets, and therefore optimum torque/ampere ratio is obtained if the armature current is composed only of its torque component. In other words, the controller should control the machine in such a way that the i_d component of the armature current is zero, while the i_q component is proportional to the desired torque.This principle can be graphically observed by looking at Figure 4.5. The condition of maximum torque/ampere ratio will be achieved by having the armature current trajectory along the iq axis, as shown in the figure. Figure 4.5 shows examples of armature current vector. The current I_1 is in the q-axis,and therefore id is zero. I_1 then represents a typical operation point where the voltage applied to the machine is V_1, which is smaller than V_{max}. The armature current I_1 is smaller than Imax, and the machine is providing a torque T_1 at speed ω_{r1}. Notice that the same torque T_1 can be provided by the same current i_1, but with different combinations of V_1 and ω_1, i.e. lower or higher speeds can be reached by varying V_1.

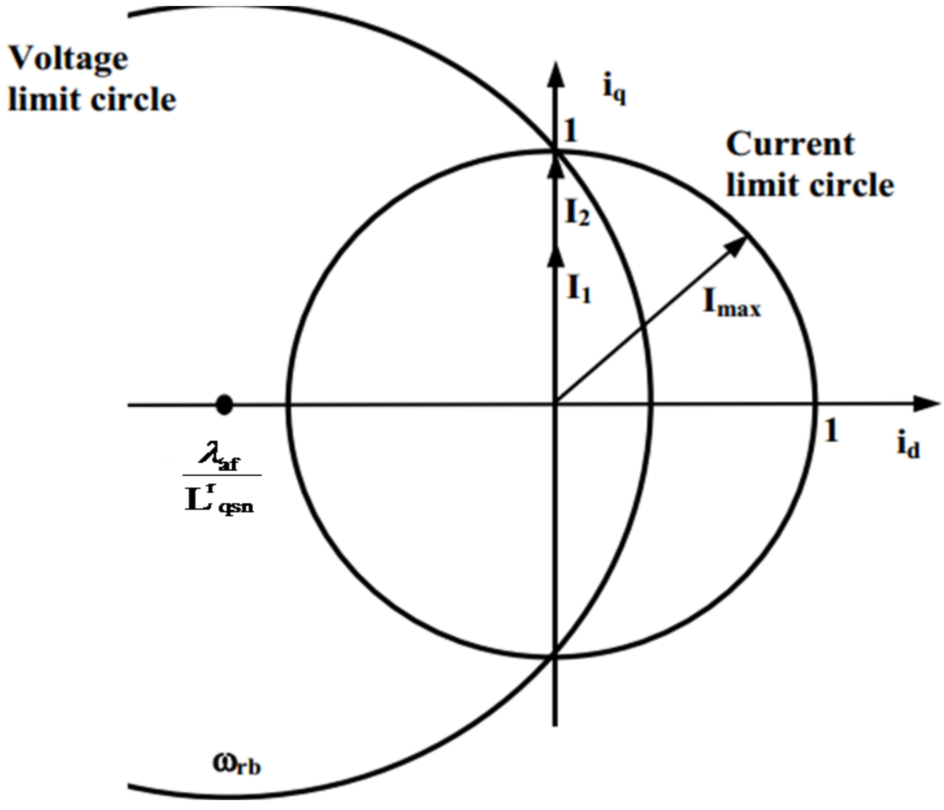

Figure 4.6: Armature current trajectory for vector control of PMSM operating in CTOR[36]

In the operating point I_2, the machine is operating at maximum or rated torque. At this point any combination of the applied voltage V_2 and speed ω_{r2} can be used.

However, there will be a speed that will allow the voltage limit circle to pass through the point where the current limit circle crosses the q-axis. This is the maximum speed where the rated torque can be developed. This speed is the aforementioned base speed ω_{rb}. The base speed is the limit of the constant torque operation range. Below this speed, the machine can provide the rated torque at any speed, but beyond this speed, the rated torque cannot be provided any longer, and this is the beginning of the constant power operation region. It is important to notice that in general the base speed is defined as the speed where the maximum circle voltage is provided by square-wave operation of the inverter. However, as mentioned before, at square-wave operation the inverter loses its ability to control the current, which is a requirement for VC and fast dynamic response of the system. Therefore, for vector control, the maximum voltage circle is defined in the limit of the undermodulation operation region of the inverter.

4.6 Constant Power Operation Region

As the speed increases beyond the maximum speed, the voltage limit circle passes through a point where the maximum current circle crosses the i_q axis, the voltage limit circle shrinks and the maximum torque can no longer be provided. It is important to emphasize that before this point the current command id was zero and the current command i_q was proportional to the desired torque. However, from this point on, although the current limit may not be violated, the controller cannot control the current in a way that the rated torque is provided, and the command currents i_d and i_q must be changed.

There are many different ways to control the id and iq currents. For instance, consider that the current command will be controlled to be in the limit of the voltage limit circle, and inside the current limit circle; however, optimum torque/ampere ratio is desired and therefore id will be controlled to be zero. Figure 4.6 shows three operation points for speeds ω_{r1}, ω_{r2}, and ω_{r3} with this control strategy. Notice that as the speed increases from r1 to r2, and from r2 to ω_{r3}, and the voltage limit circle shrinks, and therefore the maximum torque that can be developed also decreases. At speed ω_{r3}, the voltage limit circle is tangent to the i_q axis and the machine cannot provide any torque at this speed or higher. Therefore, if the current command trajectory is along the i_q axis, the range above base speed in which the machine can provide torque is very narrow.

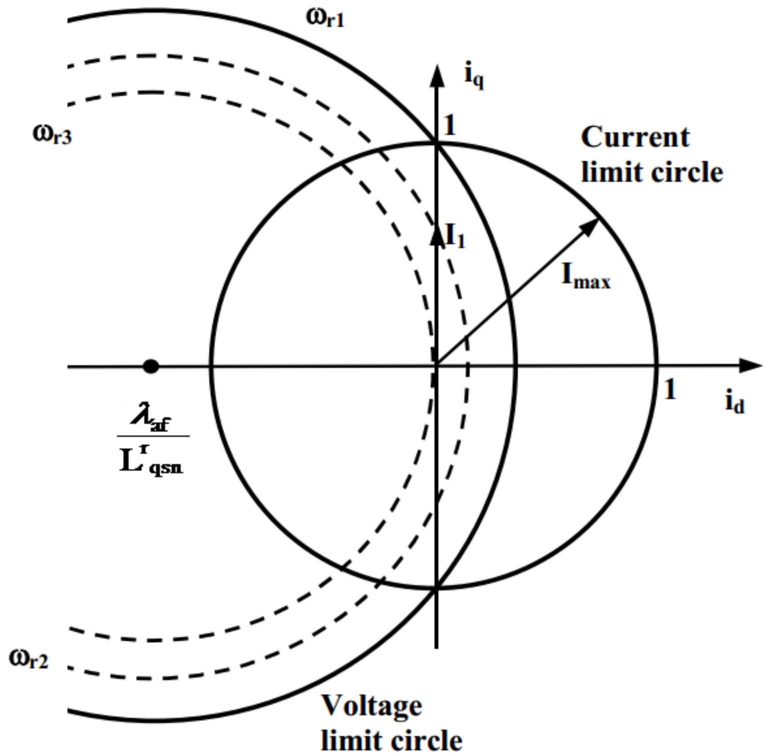

Figure 4.7: Armature current trajectory for vector control of PMSM operating in CPOR with $i_d = 0$[36]

Consider as an alternative for the previous current command trajectory, the trajectory that does not keep the id component of the command current zero. A possible current trajectory as the speed increases is along the current limit circle. Figure 4.7 shows this trajectory. In this trajectory, the i_d component of the current command increases negatively. In order to stay within the current limit circle, the i_q component must decrease, which causes the developed torque to decrease. However,in this way the decreasing rate of the torque as the speed increases is smaller,meaning that the range that the machine can operate above base speed is wider. The armature current vectors I_1, I_2, and I_3 are examples of the currents in this trajectory. Notice that they have nonzero i_d and i_q components, unlike the previous trajectory. In this case the optimum torque/ampere is not achieved anymore. However torque can be developed at higher speeds.

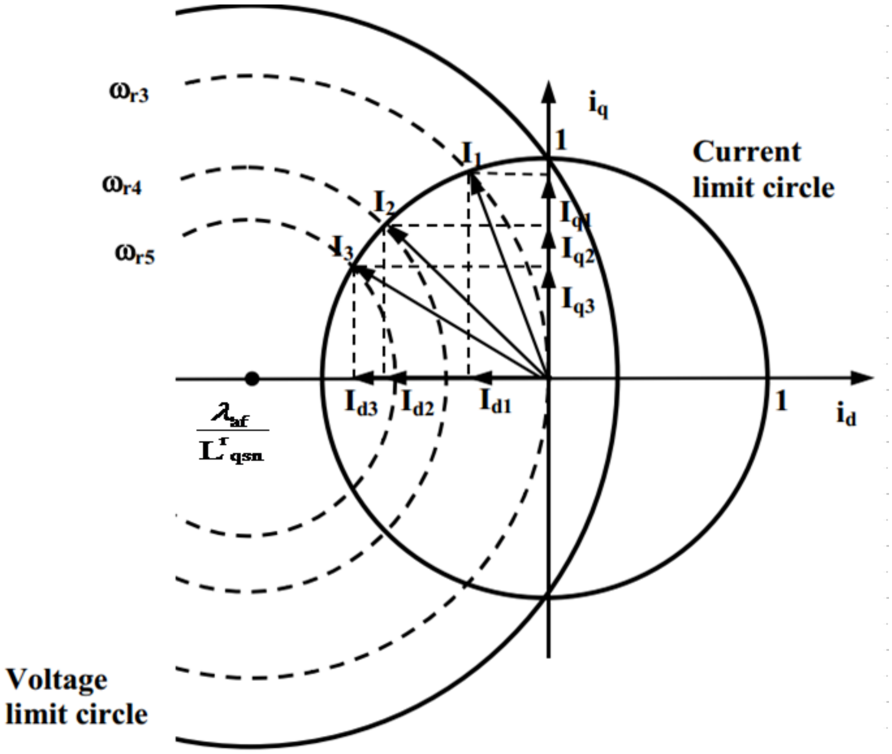

Figure 4.8: Armature current trajectory for vector control of PMSM operating in CPOR with field weakening

For instance, as shown in Figure 4.7, if the machine is required to operate at speed ω_{r3}, by using the trajectory along the q-axis,there would not be any i_q current, and therefore the machine would not be able to develop any torque. On the other hand, if the trajectory along the current limit circle is used, as shown in Figure 4.7, the I_q current would be I_{q3} and a considerable amount of torque would be developed.The objective of the field weakening technique is then to control i_d and i_q current in such way that the machine can develop constant power.

4.7 Selection of Power Rating of an Electric Motor for Electric Vehicles

The electric vehicle has many components like charging module, converters,controllers, batteries, electric motor and the block diagram of power flow in an electric vehicle is shown in Figure-4.9.

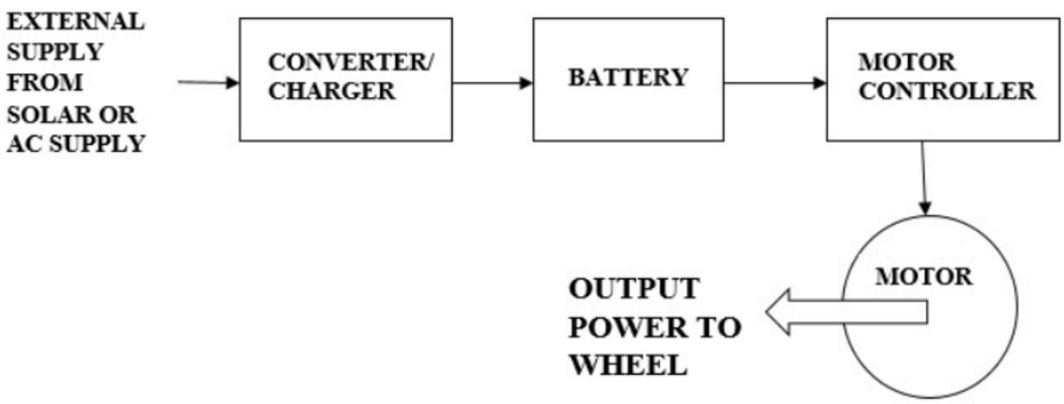

Figure 4.9: Block diagram of power flow in an electric vehicle

From the Figure-4.9, the AC power supply can be obtained externally by using solar panels to generate electricity or from domestic AC supply in chagrining station.This power is then rectified using converter and is made available to the battery through charging module. The battery supplies electric power to the motor through a motor controller, which helps in controlling the input and output parameters of the motor.The output mechanical power from the motor is given to the wheel through a drive shaft.Therefore, it is clear that an electric motor determines the output characteristics of vehicle as a whole in terms of power, torque, speed, etc. The electric motor selected for driving a vehicle must have the ability to provide sufficient power and torque to overcome the force due to load and other opposing forces acting on the vehicle.

4.7.1 Power Rating Based on Vehicle Dynamics

For deciding the power rating of a vehicle, the vehicle dynamics like rolling resistance, gradient resistance, aerodynamic drag, etc. has to be considered. For illustration procedure for selecting motor rating for an electric car of gross weight 348 kg is considered. The force required for driving a vehicle is calculated below[]

$$F_{total} = F_{rolling} + F_{gradient} + F_{aerodynamicdrag} \tag{4.21}$$

Where:

F_{total} =Total force

$F_{rolling}$=Force due to Rolling Resistance

$F_{rolling}$=Force due to Gradient Resistance

$F_{aerodynamicdrag}$=Force due to aerodynamics drag

F_{total} is the total tractive force that the output of motor must overcome.

A.Rolling Resistance

Rolling resistance is the resistance offered to the vehicle due to the contact of tires with road. The formula for calculating force due to rolling resistance is given by equation (2):

$$F_{rolling} = C_{rr} * M * g \tag{4.22}$$

Where:

C_{rr} = Coefficient of rolling resistance

M=mass in kg

g= acceleration due to gravity=9.81m/s^2

For the application considered, $C_{rr} = 0.015$ and $M = 310kg$(Maximum payload) There fore,

$$F_{rolling} = 0.015 * 310 * 9.81 = 45.6 \quad N$$

Power required to over come the rolling resistance of 45.6 N is:

$$P_{rolling} = F_{rolling} * V(kmph) \tag{4.23}$$

$$P_{rolling} = 45.6 * 65km/hr * 1/3600hr/sec * 1000m/km = 0.82kw$$

Where V=velocity in Kmph

B.Gradient Resistance

Gradient resistance of the vehicle is the resistance offered to the vehicle while climbing a hill or flyover or while travelling in a downward slope. The angle between the ground and slope of the path is represented as , which is shown in Figure-4,10.

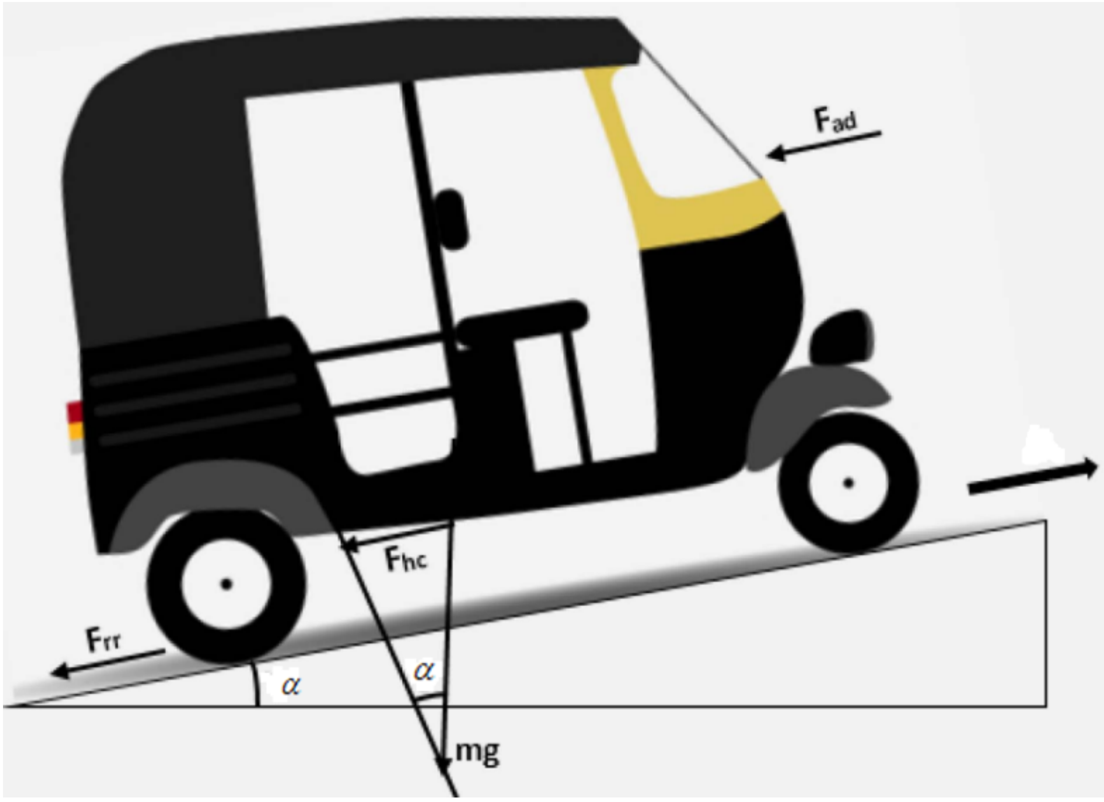

Figure 4.10: Forces Acting on a Vehicle[31]

The formula for calculating the gradient resistance is given by equation :

$$F_{gradientresistance} = \pm M * g * \sin\alpha \tag{4.24}$$

In this illustration, let us consider the electric car runs on a flat road. Therefore, the angle $\sin\alpha = 0^o$.

$$F_{gradient} = 348 * 9.81 * \sin 0^o = 0 \quad N$$

In this case, the power required to overcome gradient resistance is also zero.

C.Aerodynamic Drag

Aerodynamic drag is the resistive force offered due to viscous force acting on the vehicle.

$$F_{ad} = \frac{1}{2}\rho * A * C_d * V^2 \tag{4.25}$$

$$F_{ad} = \frac{1}{2} * 1.225 * 2.09 * 0.44 * (\frac{40000}{3600}) = 69.54 \quad N$$

Where V is the average speed of aerodynamic drag.

$$P_{ad} = 69.54 * 65 * \frac{1000}{3600} = 1.25 \quad Kw$$

It is largely determined by the shape of the vehicle. The formula for calculating the aerodynamic drag and decelerating the effect of force due to inertia also acts. In this illustration, let us consider the power required to overcome Aerodynamic drag and other resistive forces to be around 1.3 kW.
Therefore, the total tractive power required to move the vehicle is

$$P_{total} = 0.82Kw + 1.3Kw = 2.12Kw$$

But electric motor wit h output power rating of 1.92 kW should not be selected. The losses due transmission of power to the wheel must be included. Therefore, the mechanical power output ($M_{tractive}$) required to drive the vehicle is obtained as

$$M_{tractive} = \frac{P_{total}}{\eta} \tag{4.26}$$

Where,η =efficiency of the transmission gear system Let us consider the efficiency of the transmission system to be 0.85. Therefore the mechanical power output required is:

$$M_{tractive} = \frac{2.12}{0.85} = 2.49 \approx 2.5Kw$$

For the selection of power rating for an electric car of 310 kg maximum payload capacity, a motor with output power rating of 2.5 kW selected. power rating required to drive an electric vehicle of particular load is calculated.

4.8 Current and Speed controller

4.8.1 Current Controller

The design of the current for PMSM drives becomes crucial in high-performance applications. The design procedure to synthesize and implement current controllers is very similar to the high-performance current controllers in induction motor drives. Before moving on to further details, the process of the current control in the PMSM is first examined to gain an understanding of the interaction of the machine, the inverter, and the current controller. Consider the gain of the inverter to be K_r and its time constant to be T_r, which is equal to half of the time period of the PWM carrier frequency. If the desired performance of the current control loop is to resemble a first-order lag system given by

$$\frac{i_{ds}^{r}}{i_{ds}^{r*}} = \frac{K_i}{1 + sT_i} \tag{4.27}$$

where

K_i is the feedback gain of the current sensor

T_i is the desired lag

i_{ds}^{r} and i_{ds}^{r*} are d-axis winding current in rotor reference frames and their references, respectively

The current loop transfer function from Figure 4.11 as

$$\frac{i_{qs}^{r}(s)}{i_{qs}^{r*}(s)} = \frac{K_a K_t(1 + T_m s)}{H_c K_a K_r(1 + sT_m) + (1 + sT_r)\left\{K_a K_b + (1 + sT_a)(1 + sT_m)\right\}} \tag{4.28}$$

where

$$K_a = \frac{1}{R_s}; \quad T_a = \frac{L_q}{R_s}; \quad K_m = \frac{i}{B_r}; \quad T_m = \frac{J}{B_i}; \quad K_b = K_t K_m \lambda_{af} \tag{4.29}$$

The following approximations are valid near the vicinity of crossover frequency:

$$1 + sTr \cong 1 \tag{4.30}$$

$$1 + sT_m \cong sT_m \tag{4.31}$$

$$(1 + sT_a)(1 + sT_r) \cong 1 + s(T_a + T_r) \cong 1 + sT_{ar} \tag{4.32}$$

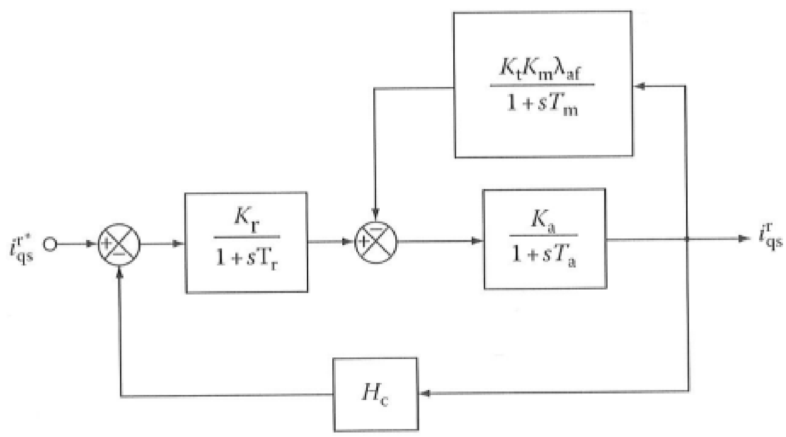

Figure 4.11: Current Controller [3]

where

$$T_{ar} = T_a + T_r \tag{4.33}$$

with this the current loop transfer function is approximated as

$$\frac{i_{qs}^r(s)}{i_{qs}^{r*}(s)} = \frac{(K_a K_t T_m)s}{K_a K_b + (T_m + K_a K_t T_m H_c)s + (T_m T_{af})s^2} \tag{4.34}$$

$$\cong \left(\frac{T_m K_r}{K_b}\right) \frac{s}{(1+sT_1)(1+sT_2)} \tag{4.35}$$

It is found that $T_1 < T_2 < T_m$ and hence ,on further approximation that, $(1 + sT_2) \cong sT_2$.The approximation current loop transfer function is then given by

$$\frac{i_{qs}^r(s)}{i_{qs}^{r*}(s)} \cong= \frac{K_i}{(1+sT_i)} \tag{4.36}$$

Where

$$K_i = \frac{T_m K_r}{T_2 K_b} \quad T_i = T_1 \tag{4.37}$$

4.8.2 Speed Controller

The speed loop is shown in Figure 4.12. Near the vicinity of Cross over frequency, the following approximation are valid: $H_w = 0.05$ V/V and $H_r = 0.8$ V/A

Maximum control voltage V_{cm} 10 v

$$(1 + sT_m) \cong sT_m \tag{4.38}$$

$$(1 + sT_i)(1 + sT_w) \cong 1 + sT_{wi} \tag{4.39}$$

$$1 + sT_w \cong 1 \tag{4.40}$$

Where

$$T_{wi} = T_w + T_i \tag{4.41}$$

The speed loop transfer function is given by

$$GH(s) = \frac{K_i K_m H_W}{T_m} \frac{K_s}{T_s} \frac{(1+sT_s)}{s^2(1+sT_{wi})} \tag{4.42}$$

From which the closed loop transfer function is obtained as

$$\frac{\omega_r(s)}{\omega_{r*}(s)} \cong \frac{1}{H_w} \left\{ \frac{K_g \dfrac{K_s}{T_s}(1+sT_s)}{s^3 T_{wi} + s^2 + K_g \dfrac{K_s}{T_s}(1+sT_s)} \right\} \tag{4.43}$$

where

$$K_g = \frac{K_i K_m K_t H_w}{T_m} \tag{4.44}$$

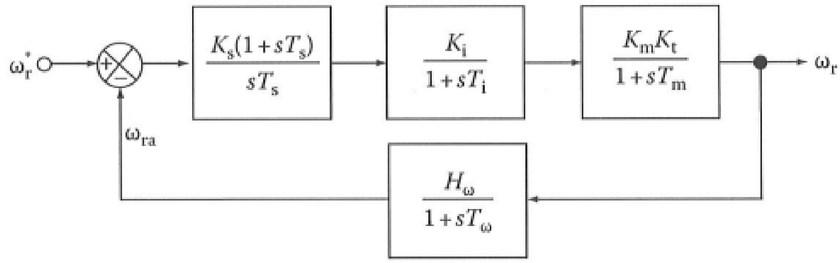

Figure 4.12: Simplified Speed Controller[3]

$$\frac{\omega_r(s)}{\omega_r^*(s)} \cong \frac{1}{H_c} \frac{(1+sT_s)}{1+(T_s)s+\left(\frac{3}{8}T_s^2\right)s^2+\left(\frac{1}{16}T_s^3\right)s^3} \tag{4.45}$$

Equating the cofficients of Equation 4.43 and 4.45 and solving the constants, yields the time and gain constants of the speed controller as

$$T_s = 6T_{wi} \quad andK_s = \frac{4}{9K_gT_{wi}} \tag{4.46}$$

Hence,the proportional gain, K_{ps}, and integral gain K_{is},. of the speed controller are derived as

$$K_{ps} = K_s = \frac{4}{9K_gT_{wi}} \tag{4.47}$$

$$K_{is} = \frac{1}{27K_gT_{wi}^2} \tag{4.48}$$

Inverter: Gain,$K_r = 0.65\frac{V_{dc}}{V_{cm}} = 18.525V/V$
Time constant, $T_r = \frac{1}{2f_c} = 0.000025s$

$$G_r(s) = \frac{K_r}{1+sT_r} = \frac{18.525}{1+0.000025s}$$

Motor(electrical):Gain, $K_a = \frac{1}{R_s} = 0.7143$; Time Constant , $T_a = \frac{L_q}{R_s} = 0.0064s$

$$G_a(s) = \frac{K_a}{1+sT_a} = \frac{0.7143}{(1+0.0064s)}$$

Torque constant, $K_t = \frac{3}{2}\left(\frac{p}{2}\right).\lambda_{af} = 2.087N.m/A$
Mechanical gain,$K_m = \frac{J}{B_r} = 100rad/s/N.m$

$$G_b(s) = \frac{K_tK_m\lambda_{af}}{(1+sT_m)} = \frac{32.26}{(1+0.6s)}$$

where the mechanical time constant is

$$T_m = \frac{J}{B_t} = 0.12s$$

Motor (Mechanical)$G_m(s) = \frac{K_m K_t}{(1 + sT_m)} = \frac{208.7}{(1 + 0.12s)}$ From Equation 4.34 and 4.35 we can drive $T_1 and T_2$ as

$$T_2 + T_1 = \frac{T_m}{K_a K_b} + \frac{K_r T_m H_c}{K_b} \tag{4.49}$$

$$T_1 * T_2 = \frac{T_m T_{ar}}{K_a K_b} \tag{4.50}$$

Solving for T_1 and T_2 gives

$$T_1 = 0.00923s$$

$$T_2 = 3.01s$$

The simplified current loop transfer function: $G_{is} = \frac{K_i}{(1 + sT_1)}$

$$T_i = T_1 = 0.00923s$$

$$K_i = \frac{T_m K_r}{T_2 K_b} = 2.4$$

Speed controller:

$$K_G = K_i K_m K_t \frac{H_w}{T_m} = 19.9$$

$$T_{wi} = T_w + T_i = 0.0123S$$

$$T_s = 6T_{wi} = 0.0738s$$

$$k_{ps} = \frac{4}{9 * k_g T_{wi}} = 2.2$$

$$k_{is} = \frac{1}{27 k_g T_{wi}} = 12$$

The base value Calculated as:

$I_b = 12A, P_b = 2.5kw, T_b = 6N.m$

Base voltage,$V_b = \frac{P_b}{3I_b} = \frac{2500}{3 * 12} = 70V$

Base speed $\omega_b = \frac{P_b}{T_b} = \frac{2500}{6} = 416.6rad/s$

Base impedance, $Z_b = \frac{V_b}{I_b} = \frac{70}{12} = 5.8\Omega$

Base inductance, $L_b = \frac{Z_b}{\omega_b} = \frac{5.8}{416.6} = 0.014$

Normalized Stator resistance $R_{sn} = \frac{R_s}{Z_b} = \frac{1.4}{5.83} = 0.24p.u$

Stator phasor voltage , V_s is equal to the peak value of the stator phase voltage ,and it is calculated as:

$$V_s = 0.55V_{dc} = 0.55(285) = 156.75$$

Its normalized value ,$V_{sn} = \dfrac{V_s}{V_b} = \dfrac{156.75}{70} = 2.23p.u.$

4.9 Simulation Results of Vector Control of PMSM with Field Weakening Operation

4.9.1 Simulation Result and Discussion

This section deals with the simulation results of PMSM drive system. The parameters of the motor that are used in the simulation are shown in table 1(APP-I) . The system built in Matlab for a PMSM drive system has been simulated at the constant torque and fluxweakening regions of operation.

In the simulation of the surface mounted PMSM both constant torque and fluxweakening region have been showed using the software packageMATLAB for wide speed range operation of pmsm for electric vehicle application.The motor is operated with constant torque up to its base speed and beyond the base speed flux-weakening mode is initialized.

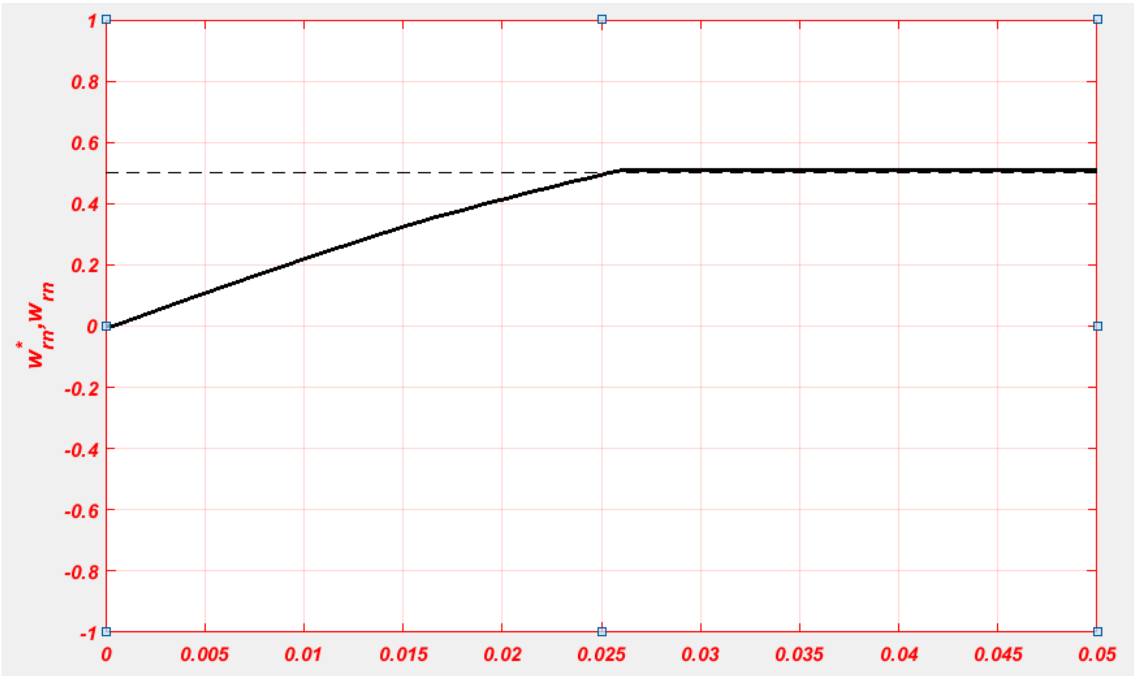

Figure 4.13: Rotor Speed of SPMSM

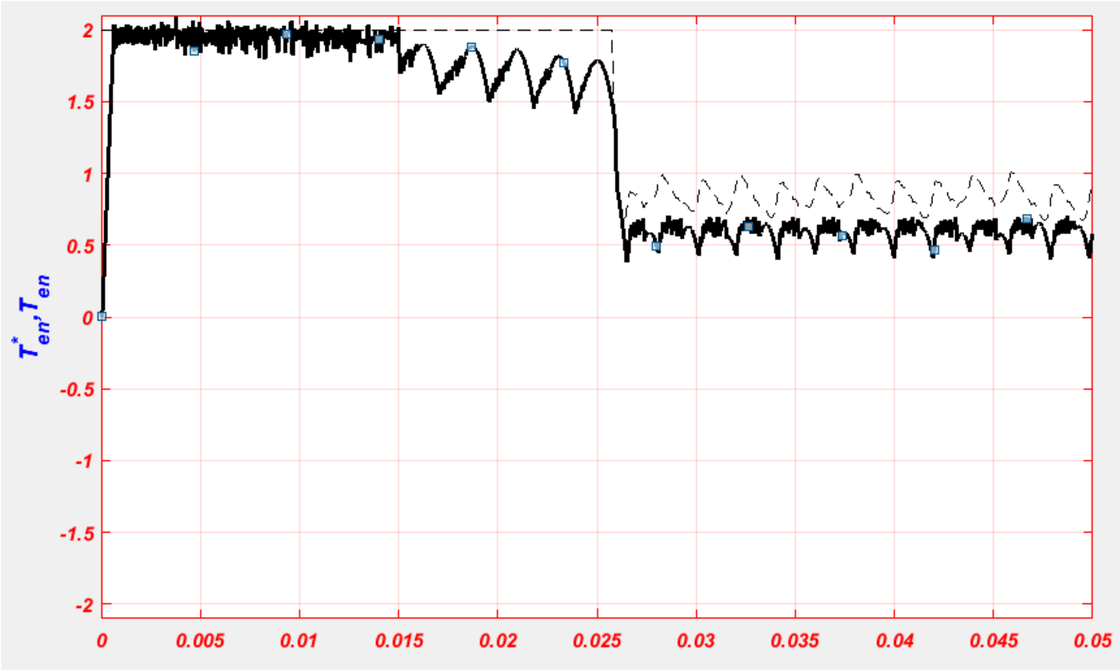

Figure 4.14: Developed Torque

A flux weakening operation is shown in Figure-4.17.Above 0.3 p.u.,flux weakening is initiated using the algorithm.The d-axis current reference is reduced during flux weakening, resulting in a reduction of air gap flux linkages.During flux weakening ,the torque command is reduced to maintain the constant air gap power.

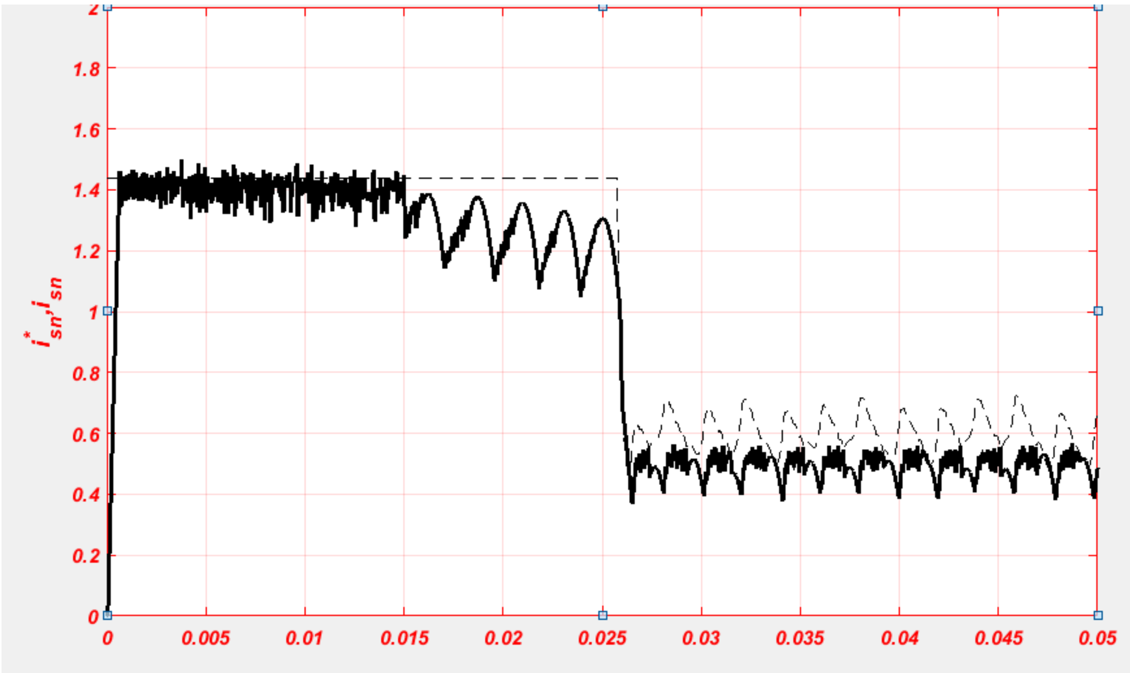

Figure 4.15: Stator current

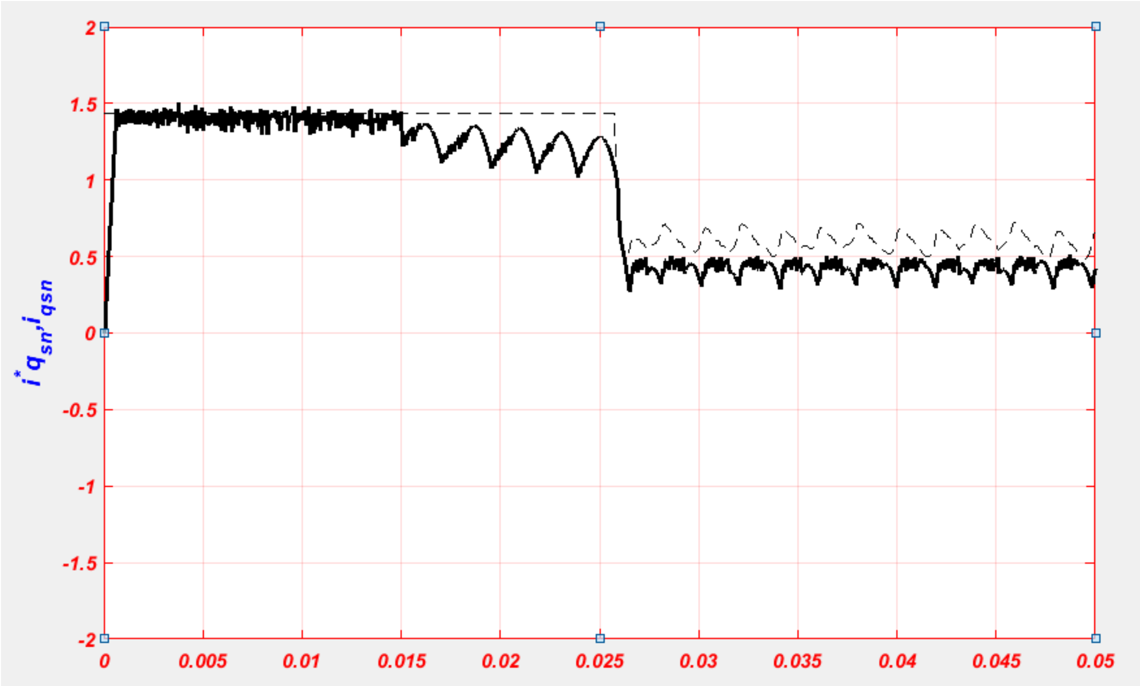

Figure 4.16: Torque producing current(q-axis current)

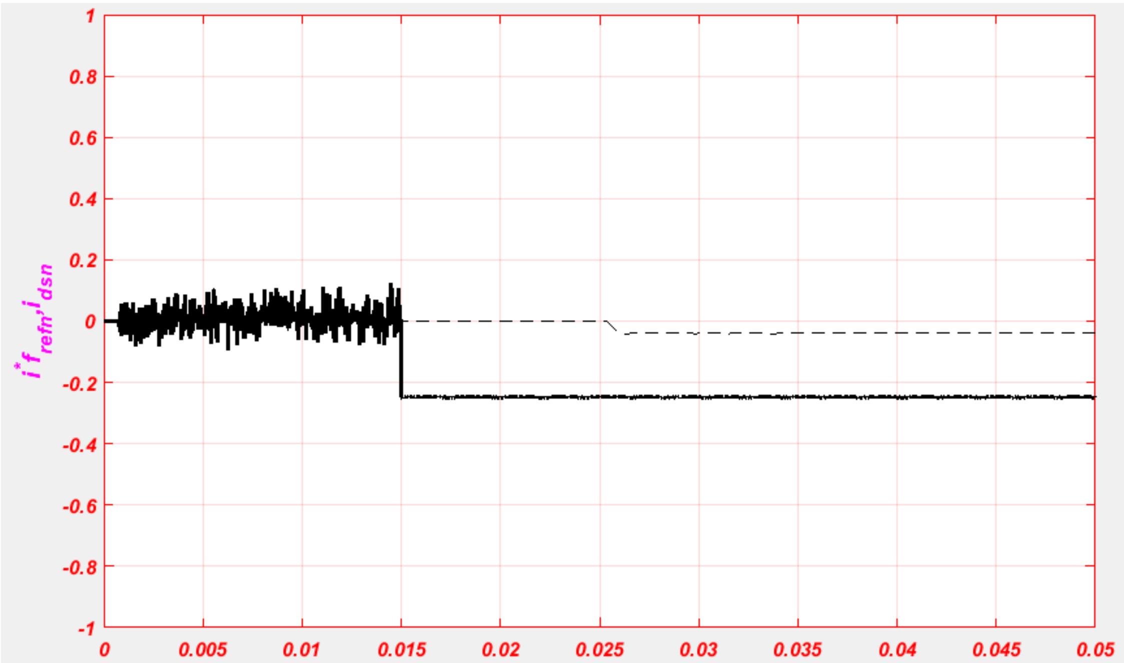

Figure 4.17: Flux producing current(d-axis current)

As the speed increases and reaches at base speed ,at this point the current command i_d is not longer zero and becomes negative due to air gab flux weakened . ‘The current command i_q proportional to the desired(rated) torque have started deceased as well because of the current constraint must be satisfied.Due to this the developed torque decrased as well since torque is entirely produced by i_q current.

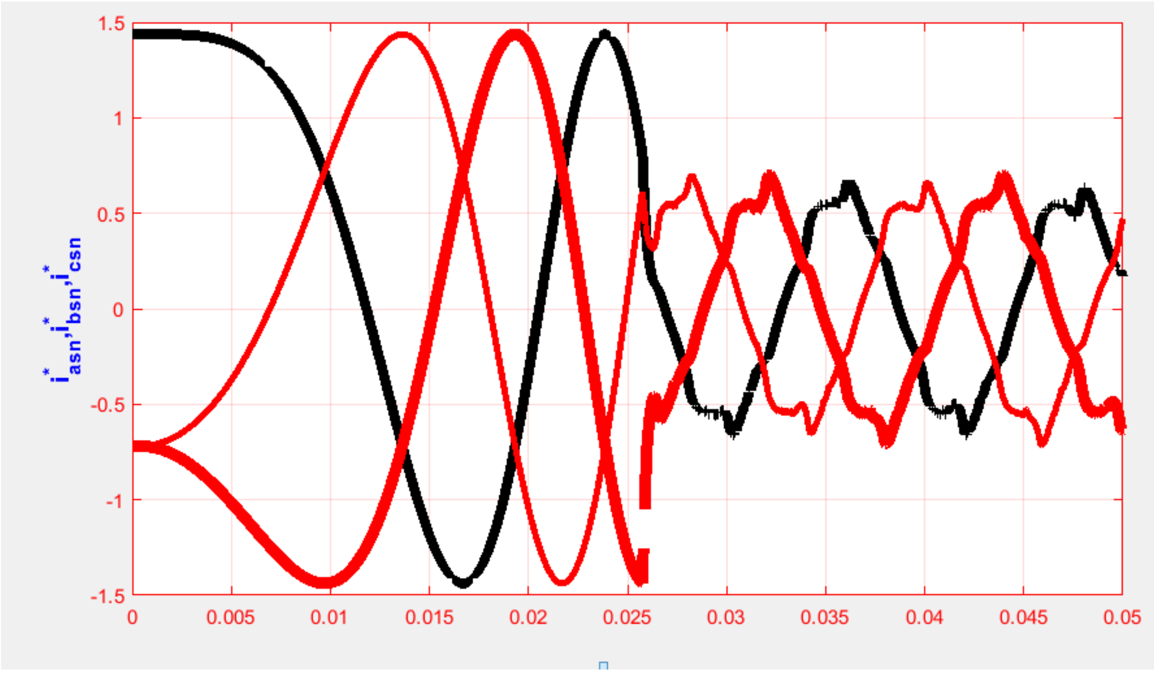

Figure 4.18: Reference stator current

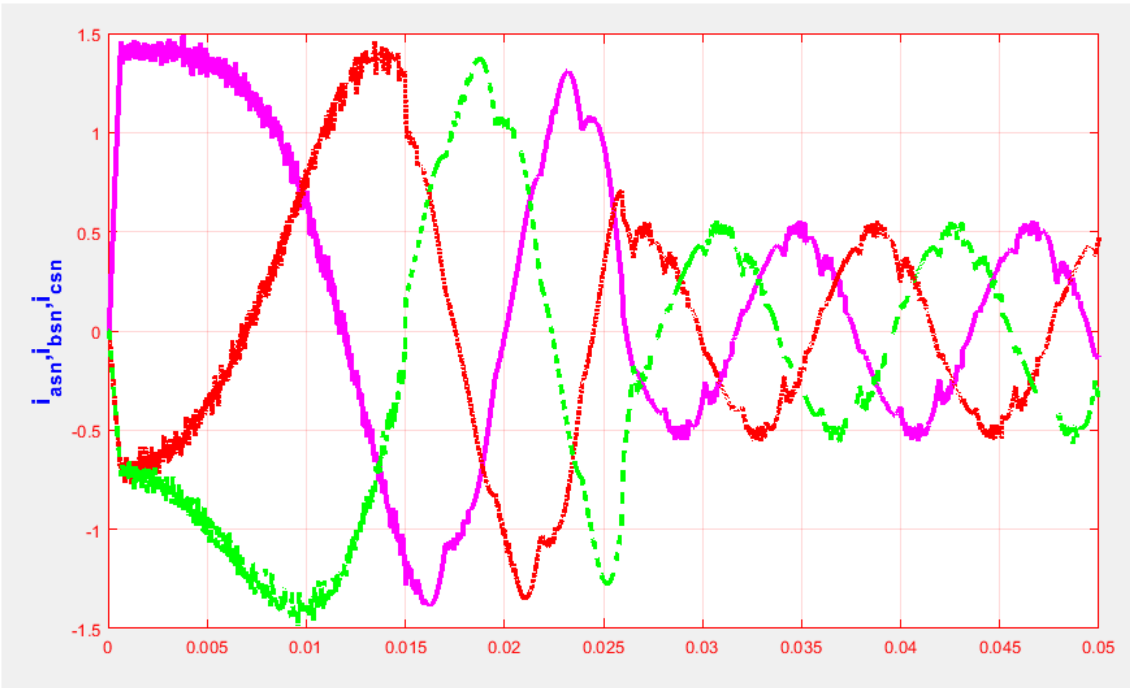

Figure 4.19: Actual stator current input to the PMSM

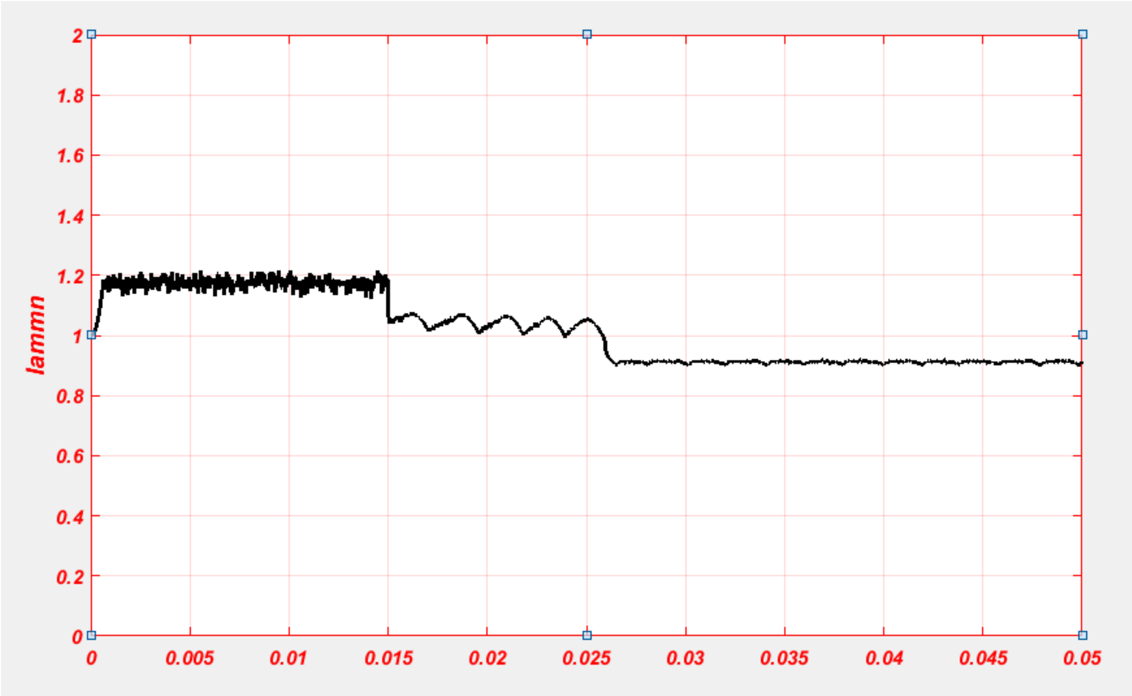

Figure 4.20: Air gab(mutual flux linkage) flux

Due to negative stator current injected the air gab flux as the result is weakened as shown from figure 4.20.This weakened air gap flux control the back emf induced due to rotor flux and maintained constant as the speed increased beyond base speed.

CHAPTER 5:

CONCLUSIONS AND RECOMMENDATION

5.1 Conclusion

The objective of this work is to explain and analyze Vector control of field weakening for wide speed range application of PMSM drive system for Electric vehicle (EV).Field weakening control has been developed and operation below and above rated speed has been studied. The dynamic performance of flux/field weakening control of PMSM motors has been studied. The demagnetizing effect of the negative direct current to weaken the air gap flux was presented in detail. Vector control of PMSM with field weakening was discussed and Analysis of the operation limits of the system have been completed. This analysis considers the voltage and current limits. The result of this analysis showed that the constant power operation range of the PMSM when using VC with field weakening technique the toque reduced from rated value while the speed increased beyond base speed and air gap flux reduced and becomes negative due to negative d-axis current.The torque producing current was decreased in flux weakening region and at the result torque reduced from rated value at base speed. The field weakening has not been implemented using DSP due to time constraint and some technical problems on the DSP used.

5.2 Recommendation

The main recommendations for this Thesis are summarized as:

- The main drawbacks of using speed/position sensor are high cost, lower system reliability and special attention to noise. Such problems make sensorless drives popular.So sensor less control scheme recommended in future work.
- Due to unavailability of different device component(DSP,sensor,...) locally It was a challenge to analysis the system experimentally.
- Using space vector technique it is possible to develop farther for multilevel inverter just like three level, five level, seven level and etc. To get smooth steady state speed of PMSM.

REFERENCES

[1] Peter O. Rasmussen and Torben N. Matzen (2009) Torque Control in Field Weakening Mode Alborg University Institute of Energy Technology

[2] Ruiwu, C.; Chris, M.; Ming, C.(2012) Quantitative Comparison of Flux-Switching Permanent-Magnet Motors,Published in IEEE Transactions on Magnetics.

[3] R. Krishnan (2001), Electric Motor Drives - Modeling, Analysis, and Control. Prentice Hall .

[4] Navid Maleki, Mohammad Reza Alizadeh Pahlavani, Iman Soltani (2015). A Detailed Comparison Between FOC and DTC Methods of a PMSM Drive. Journal of Electrical and Electronic Engineering.Vol. 3, No. 2-1, pp. 92-100.

[5] Adrian BLANU, Leonard Marin FLOREA (2013), Comparison of Electric Motor used for Electric Vehicles Propulsion.Faculty of Electrical Engineering, University Politehnica of Bucharest, Romania.

[6] B. K. Bose (2002), Modern Power Electronics and AC Drives: Prentice Hall.

[7] Ahmed A. AbdElhafeza,b*, Majed A. Aldalbehia, (2017), Comparative Study for Machine Candidates for High Speed Traction Applications,Assiut University, Assiut, Egypt.

[8] STULRAJTER, M.HRABOVCOVA, V.FRANKO, M. (2007) Permanent Magnets Synchronous Motor Control Theory, Journal of Electrical Engineering 58 No. 2 7984.

[9] G. Pellegrino, B. Boazzo, and T. M. Jahns,(2014) Direct flux control of PM synchronous motor drives for traction applications, in IEEE Transportation Electrification Conference and Expo (ITEC), pp. 16.

[10] M.F. Moussa, A. Helal, Y. Gaber, and H.A. Youssef (2008), Unity power factor control of permanent magnet motor drive system, 12th International Middle-East Power System Conference, pp 360-367.

[11] V. R. Jevremovic and D. P. Marcetic (2008), Closed-loop flux-weakening for permanent magnet synchronous motors, 4th IET Conference on Power Electronics, Machines and Drives, pp. 717-721.

[12] W. L. Soong and N. Ertugrul (2012), Field-weakening performance of interior permanent magnet motors, IEEE Trans. Ind. Appl., vol. 38, no. 5, pp. 1251-1258.

[13] Q. Liu,(2005) Analysis, design and control of permanent magnet synchronous motors for wide-speed operation, Ph. D. dissertation, National University of Singapore.

[14] BajajRE2SAuto-rickshaw Technical Specification [online available], http://www.bajajauto.com.

[15] S. Chattopadhyay, M. Mitra, and S. Sengupta,(2011) Electric Power Quality, ser. Power Systems. Springer London, Limited. [Online]. Available: http://books.google.it/books?id=Ip0kfBI2ELcC

[16] M. Bodson, J. Chiasson, L. Tolbert, (2001)"A Complete Characterizations of TorqueMaximization for Permanent Magnet Non-salient Synchronous Motor", IEEE American Controls Conference, June 25-27, , Arlington, Virginia.

[17] Q. Lei, S. Yang, F. Z. Peng, and R. Inoshita,(2009) Application of Current-fed QuasiZ-Source Inverter for Traction Drive of Hybrid Electric Vehicles, Vehicle Power and Propulsion Conference, pp. 754-760,.

[18] Walzer, P., (1983)"Future propulsion systems for cars, Resources and Conservation, Vol. 10, pp. 49-64.

[19] Vezzini, A., Sharan, H, and Umanand, L, (2005)"Low-pollution three-wheeler autorickshaw with power-assist series hybrid and novel DC-link voltage system, Journal of Indian Institute of Science, Vol. 85, March-April, pp. 105-118.

[20] G. Foo and X. Zhang,(2017) Robust direct torque control of synchronous reluctance motor drives in the field-weakening region, IEEE Transactions on Power Elect, vol. 32, no. 2, pp. 1289-1298.

[21] Dawit Endeshaw and Bezawit Admasu,(2016),A Hike on Price, Demand for Three Wheeler Vehicles,Fortune Writers,Published on Dec 06[VOL 17 ,NO 866]

[22] A. Susperregui, M. Martinez,(2012) I. Zubia, and G. Tapia, Design and tuning of fixed-switching-frequency second-order sliding-mode controller for doubly fed induction generator power control, IET Electric Power Applications, vol. 6, pp. 696-706.

[23] Matti Eskola, (2006) Speed and Position Sensorless Control of Permanent Magnet Synchronous Motors in Matrix Converter and Voltage Source Converter Applications, Ph.D. dissertation, Tampere University of Technology, Tampere.

[24] M. F. Rahman, L. Zhong, and K. W. Lim,(2015) A direct torque-controlled interior permanent magnet synchronous motor drive incorporating field weakening, IEEE Transaction on Industry Application; vol. 34,pp.1246-1253.

[25] C. E. Moucary, E. Mendes, and A. Razek,(2002) Decoupled direct control for pwm inverter-fed induction motor drives, IEEE Transaction on Industry Applications, vol.38,pp. 1307-1315.

[26] B. Cui, J. Zhou, and Z. Ren, "Modeling and simulation of permanent magnet synchronous motor drives," 2001.

[27] F. Boriz, A. Diez, M.W.Dagner, and R. D. Lorenz,(2001) Current and Flux Regulation in Field Weakening Operation, IEEE Trans. Indust .Applicat, vol 37, No 1, pp 42-49.

[28] Daniel Fita (2005) "Fild Weakening Control of PMSM"Thesis Report, Addis Ababa University.

[29] N. P. Quang and J.-A. Dittrich.(2008), Vector Control of Three-Phase AC Machines: System Development in the Practice (Power Systems). Springer.

[30] Florian Demmelmayr, Markus Troyer, Manfred Schroedl,(2010) Advantages of PM-machines Compared to Induction Machines in Terms of Efficiency and Sensorless Control in Traction Applications,Vienna University of Technology, Vienna, Austria.

[31] Mishra, Prasun, Suman Saha, and H. P. Ikkurti.(2013) "A Methodology for Selection of Optimum Power Rating of Propulsion Motor of Three Wheeled Electric Vehicle on Indian Drive Cycle (IDC)." International Journal on Theoretical and Applied Research in Mechanica/ Engineering, vol.2, no.l, pp. 95-109.

[32] R. Krishnan,(1993) Control and Operation of PM Synchronous Motor Drives in the Field Weakening Region, Proceedings of the IEEE International Conference on Industrial Electronics, Control, and Instrumentation, IECON.

[33] M. Zordan, P.Vas, M. Rashed, S. Bolognani, and M. Zigliotto,(2016) Field-Weakening in High-Performance PMSM Drives: A Comparative Analysis,IEEE Industry Applications Conference, Rome.

[34] Tesfaye Getnet (2018), Bajaj in Addis to have fixed tariff based on new study, Capital news paper,Addis Ababa,January 29.

[35] J. Lara, J. Xu, and A. Chandra,(2016) Effects of rotor position error in the performance of field-oriented-controlled pmsm drives for electric vehicle traction applications, IEEE Transaction on Industrial Electronics, vol.63, no.8, pp.4738-4751.

[36] Muyang Li,(2009) Flux-Weakening Control for Permanent-Magnet Synchronous Motors Based on Z-Source Inverters ,Master's Theses,Marquette University.

APPENDIX I

Table 1 Three-tiyer Vehicle Specification used[14]

Overall length (mm)	2625
Overall width (mm)	1300
Overall height (mm)	1710
Wheel base (mm)	2000
Ground Clearance (mm)	180
Turning radius (m)	2.88
Tyres	4.00-8,4PR
Roll resistance,μ_{rr}	0.015
Air drag coefficient,C_d	0.44
Frontal Surface Area,A (m^2)	2.09

Fig 1 A three-wheeled Bajaj

Table 2 Physical Specification of Engine

Parameter	**Value**
Type	Four stroke,SI,Forced air cool
Weight	45Kg
No. of Cylinder	one
Displacement	173.52cc
Maximum Speed	5000Rpm
maximum Torque	12 NM
Maximum Pay load	310kg
Average pay load	100Kg

Table 3 PMSM drive system Parameter

λ_{af}	0.1546 wb-Turn
$L_q = L_d$	0.0056 H
R_s	1.4 Ω
Rated current	12 A
moment of inertia(J)	0.0012 kg m^2
Number of pole(P)	6
Switching (carrier) frequency of inverter (f_c)	20 kHz
Dc link voltage input to the inverter	285 v
Friction coefficient B_l	0.01 N.m/rad/s

APPENDIX II

```
clear all; close all;
%Machine Parameters
p=6;                    %number of pole
Rs=1.4;                 %stator resistance
Ld=0.0056;               %d axis inductance
Lq=0.0056;               %q axis inductance
lamaf=.1546;            %rotor flux linkage
B=0.01;                 %friction coefficient
J=0.0012;               %moment of inertia
vdc=285;                %Dc link voltage
wr_ref=523.6;           %MAximum speed
%converter and controller parameter
%converter and controller parameter

fc=20000;           %PWM switching frequency
kpi=12;             %proportional gain of spped controller
kp=2.2;               %proportional gain of spped controller
ki=4;               %Integral gain of current controller

%Base values
 Tb=6;
 Ib=12;
 Vb=70;
 Lb=0.014;

 Wb=416.6;
 ias=0;ibs=0;ics=0;tl=0;
```

```
%Initial parameters

theta_r=0;            %Initial position
wr=0;                 %Initial speed
t=0;                  %Initial time
dt=1e-6;              %Integration Time step
tfinal=.07;           %final time
if_ref=-1e-16;        %set d axis current to small negative value
iqs=0;ids=0;
vqs=0;vds=0;
Tl=0.3*Tb;         %load torque value
n=1;
x=1;
signe=1;
ramp=-1;
ias=0;ibs=0;ics=0;
tl=0;
vax1=0;vbx1=0;vcx1=0;
zia=0;zib=0;zic=0;

%simulation starts here

while(t<tfinal),
```

```
while(t<tfinal),

    wr_err=wr_ref-wr;     %speed error
    y=y+wr_err*dt;        %speed PI controller
    Te_ref=kp*wr_err+ki*y;


   if wr<wb/2,
        fwr=1;
    end
    if wr>wb/2,
        fwr=(wb/2)/wr;
    end
    Te_refnew=Te_ref*fwr;
    if_ref=(fwr-1)*lamaf/Ld;
    it_refnew=Te_refnew*(2/3)*(2/p)/((Ld-Lq)*if_ref+lamaf);

    %LIMITER
    if Te_ref>2*Tb,
        Te_ref=2*Tb;
    end
     if t>0.015,

     end
%      if Te_ref<2*Tb
%          Te_ref=Te_ref*fwr;
 end
%        if Te_ref<2*Tb
%            Te_ref=Te_ref*fwr;
%        end

      %calculate reference currents
      it_refnew=Te_ref*(2/3)*(2/p)/((Ld-Lq)*if_ref+lamaf);
      is_ref=sqrt(it_refnew^2+if_ref^2);

      if it_refnew>=0,
          delta_ref=pi/2;
      elseif it_refnew<0,
          delta_ref=-pi/2;
      end

%        if wr<wb/2,
%            fwr=1;
%       end
%       if wr>wb/2,
%           fwr=(wb/2)/wr;
%       end
%       Te_refnew=Te_ref*fwr;
%       if_ref=(fwr-1)*lamaf/Ld;
%       it_ref=Te_refnew*(2/3)*(2/p)/((Ld-Lq)*if_ref+lamaf);
      %calculate reference phase currents

      ias_ref=is_ref*sin(theta_r+delta_ref);
```

```
ibs_ref=is_ref*sin(theta_r+delta_ref-2*pi/3);
ics_ref=is_ref*sin(theta_r+delta_ref+2*pi/3);

%calculate control voltage to be applied to pwm control
vax=kpi*(ias_ref-ias);
if vax>1,
    vax=1;
elseif vax<-1,
    vax=-1;
end
vbx=kpi*(ibs_ref-ibs);
if vbx>1,
    vbx=1;
elseif vbx<-1,
    vbx=-1;
end
vcx=kpi*(ics_ref-ics);
if  vcx>1,
    vcx=1;
elseif vcx<-1,
    vcx=-1;
end
%sample and hold
if t1>1/fc,
    vax1=vax;
    vbx1=vbx;
    vcx1=vcx;
    t1=0;
end
%pwm controller
if vax1>=ramp,
    vao=vdc/2;
elseif vax1<ramp,
    vao=-vdc/2;
end
if vbx1>=ramp,
    vbo=vdc/2;
elseif vbx1<ramp,
    vbo=-vdc/2;
end
if vcx1>=ramp,
    vco=vdc/2;
elseif vcx1<ramp,
    vco=-vdc/2;
end

%compute line voltage
vab=vao-vbo;
vbc=vbo-vco;
vca=vco-vao;
%compute phase voltages
```

```
vas=(vab-vca)/3;
vbs=(vbc-vab)/3;
vcs=(vca-vbc)/3;
%q and d axes voltages in rotor reference frames
vqs=(2/3)*(cos(theta_r)*vas+cos(theta_r-2*pi/3)*vbs+cos(theta_r+2*pi/3)*vcs);
vds=(2/3)*(sin(theta_r)*vas+sin(theta_r-2*pi/3)*vbs+sin(theta_r+2*pi/3)*vcs);
%machine equations to compute currents in rotor reference
%frame,and torque angle ,torque
d_iqs=(vqs-Rs*iqs-wr*Ld*iqs-wr*lamaf)*dt/Lq;
iqs=iqs+d_iqs;
d_ids=(vds+wr*Lq*iqs-Rs*ids)*dt/Ld;
ids=ids+d_ids;
is=sqrt(iqs^2+ids^2);
delta=atan(iqs/ids);      %torque angle
Te=(3/2)*(p/2)*iqs*((Ld-Lq)*ids+lamaf);    %calculate torque

%calculate speed and position
d_wr=((p/2)*(Te-Tl)-B*wr)*dt/J;
wr=wr+d_wr;
d_theta_r=wr*dt;
theta_r=theta_r+d_theta_r;
%phase currents
ias=iqs*cos(theta_r)+ids*sin(theta_r);
ibs=iqs*cos(theta_r-2*pi/3)+ids*sin(theta_r-2*pi/3);
ics=-(ias+ibs);
%PWM RAMP
ramp=signe*(2/(1/(2*fc)))*dt+ramp;
            if ramp>1,
                signe=-1;
            end
            if ramp<-1,
                signe=1;
            end
            t=t+dt;                    %Increament time
            t1=t1+dt;
            %plot variables
            if x>16,
                t
                tn(n)=t;
                Terefn(n)=Te_ref/Tb;
                it_refnewn(n)=it_refnew/Ib;
                if_refn(n)=if_ref/Ib;
                is_refn(n)=is_ref/Ib;
                ias_refn(n)=ias_ref/Ib;
                ibs_refn(n)=ibs_ref/Ib;
                ics_refn(n)=ics_ref/Ib;
                iasn(n)=ias/Ib;
                ibsn(n)=ibs/Ib;
                icsn(n)=ics/Ib;
                vasn(n)=vas/Vb;
                vbsn(n)=vbs/Vb;
                vcsn(n)=vcs/Vb;
                iqsn(n)=iqs/Ib;
                idsn(n)=ids/Ib;
```

```
            isn(n)=is/Ib;
            Ten(n)=Te/Tb;
            wrn(n)=wr/wb;
            wrrefn(n)=wr_ref/wb;
            lammn(n)=sqrt((1+Ld*ids/(Ib*Lb))^2+(Lq*iqs/(Ib*Lb))^2);
            n=n+1;
            x=1;
        end
        x=x+1;
    end
    %plotting
    figure(1);orient tall;
%   plot(4,2,3)
%   plot(tn,Terefn,'k--',tn,Ten,'k');axis([0 .05 -2.1 2.1]);
%   set(gca,'xticklabel',[]);
%   ylabel('T^*_e_n,T_e_n','FontSize',9,'FontWeight','bold','Color','b')
    subplot(4,2,5)
    plot(tn,is_refn,'k--',tn,isn,'k');axis([0 .05 0 2]);
    set(gca,'xticklabel',[]);
    ylabel('i^*_s_n,i_s_n','FontSize',9,'FontWeight','bold','Color','red')
    subplot(4,2,1)
    plot(tn,wrrefn,'k--',tn,wrn,'k');axis([0 .05 -1 1]);
    set(gca,'xticklabel',[]);
    ylabel('w^*_r_n,w_r_n','FontSize',9,'FontWeight','bold','Color','r')
    subplot(4,2,7)
    plot(tn,it_refnewn,'k--',tn,iqsn,'k');axis([0 .05 -2 2]);
    ylabel('i^*q_s_n,i_q_s_n','FontSize',9,'FontWeight','bold','Color','blue')
subplot(4,2,2)
plot(tn,if_refn,'k--',tn,idsn,'k');axis([0 .05 -1 1]);
set(gca,'xticklabel',[]);
ylabel('i^*f_r_e_f_n,i_d_s_n','FontSize',9,'FontWeight','bold','Color','g')
subplot(4,2,4)
plot(tn,ias_refn,'k',tn,ibs_refn,'k:',tn,ics_refn,'k--');
axis([0 .05 -1.5 1.5]);
set(gca,'xticklabel',[]);
ylabel('i^*_a_s_n,i^*_b_s_n,i^*_c_s_n','FontSize',9,'FontWeight','bold','Color','b')
subplot(4,2,6)
plot(tn,iasn,'k',tn,ibsn,'k:',tn,icsn,'k--');
axis([0 .05 -1.5 1.5]);
set(gca,'xticklabel',[]);
ylabel('i_a_s_n,i_b_s_n,i_c_s_n','FontSize',9,'FontWeight','bold','Color','b')
subplot(4,2,8)
plot(tn,lammn,'k');
axis([0 .05 0 2]);
ylabel('lammn','FontSize',9,'FontWeight','bold','Color','r')
```